

Surface and Interface Engineering of Zn Anodes in Aqueous Rechargeable Zn-Ion Batteries

Jiaxian Zheng, Zihao Huang, Fangwang Ming, Ye Zeng, Binbin Wei, Qiu Jiang,*
Zhengbing Qi,* Zhoucheng Wang, and Hanfeng Liang*

Rechargeable zinc-ion batteries (ZIBs) have shown great potential as an alternative to lithium-ion batteries. The ZIBs utilize Zn metal as the anode, which possesses many advantages such as low cost, high safety, eco-friendliness, and high capacity. However, on the other hand, the Zn anode also suffers from many issues, including dendritic growth, corrosion, and passivation. These issues are largely related to the surface and interface properties of the Zn anode. Many efforts have therefore been devoted to the modification of the Zn anode, aiming to eliminate the above-mentioned problems. This review gives a comprehensive summary on the mechanism behind these issues as well as the recent progress on Zn anode modification with focus on the strategies of surface and interface engineering, covering the design and application of both the Zn anode supports and surface protective layers, along with abundant examples. In addition, the promising research directions and perspective on these strategies are also presented.

1. Introduction

The rapid depletion of fossil fuels and their adverse environmental impacts have led to a strong interest in pollution-free renewable energy resources such as solar, wind, and geothermal, which are becoming increasingly essential to meet the vision of global sustainability. The intermittent nature of these clean energy sources makes energy storage devices indispensable.^[1] Lithium-ion batteries (LIBs) are among the most popular energy storage devices with high efficiency, long lifespan, high energy density, and low maintenance cost, dominating the market for decades.^[2,3] Nevertheless, the low abundance of Li on earth, the use of flammable and toxic organic electrolytes, and other safety issues severely limit the wide-

spread application of LIBs.^[4,5] In this regard, aqueous batteries based on earth-abundant materials are promising alternatives. Zn-based batteries (including Ni-Zn, Ag-Zn, Zn-MnO₂, and Zn-air batteries) with specific energy densities between 80 and 475 Wh kg⁻¹ have received tremendous attention.^[6–8] One of the most significant advantages of zinc-ion batteries (ZIBs) is the use of high-capacity Zn metal as the anode (820 mAh g⁻¹).^[9] At the same time, Zn metal delivers a high specific volumetric capacity (5855 mAh cm⁻³) compared to Na, Mg, and Li metals (Table 1), which is attractive for large-scale applications.

The charging/discharging processes of ZIBs accompanies the electron transfer according to the following reaction:



The Zn anode reaction can be divided into two processes: i) electrons transfer from Zn metal anode to the cathode through the external circuit; ii) Zn is oxidized to Zn²⁺ ion, which then diffuses to the cathode through the electrolyte. Similar to the LIBs, the ZIBs also suffer from the dendritic growth of the Zn anode, which is normally caused by the inhomogeneous Zn stripping/plating processes.^[14] The Zn deposits continue to accumulate and eventually form dendrites, which increase the risk of puncturing the battery separator and thus short circuits, leading to a short lifespan and decreased Coulombic efficiency.^[15] On the other hand, the breakage of Zn dendrites would create “dead zinc” that decreases the utilization of Zn anode. In addition, the Zn undergoes severe corrosion and


J. Zheng, Z. Huang, Y. Zeng, Z. Wang, H. Liang
State Key Laboratory of Physical Chemistry of Solid Surfaces
College of Chemistry and Chemical Engineering
Xiamen University
Xiamen 361005, P. R. China
E-mail: hfliang@xmu.edu.cn

F. Ming
Materials Science and Engineering
King Abdullah University of Science and Technology (KAUST)
Thuwal 23955, Saudi Arabia

B. Wei
Shenzhen Geim Graphene Center
Tsinghua-Berkeley Shenzhen Institute and Tsinghua Shenzhen International
Graduate School
Tsinghua University
Shenzhen 518055, P. R. China

Q. Jiang
School of Materials and Energy
University of Electronic Science and Technology of China
Chengdu 611731, P. R. China
E-mail: jiangqiu@uestc.edu.cn

Z. Qi
Key Laboratory of Functional Materials and Applications of Fujian Province
School of Materials Science and Engineering
Xiamen University of Technology
Xiamen 361024, P. R. China
E-mail: zbqi@xmut.edu.cn

 The ORCID identification number(s) for the author(s) of this article can be found under <https://doi.org/10.1002/smll.202200006>.

DOI: 10.1002/smll.202200006

Table 1. Key performance indicators of monovalent and multivalent metal ions.^[5,10–13]

Metal electrode	Standard potential (V vs SHE)	Cost [USD kg ⁻¹]	Gravimetric capacity [mAh g ⁻¹]	Volumetric capacity [mAh cm ⁻³]	Hydrated ionic radius [Å]	Abundance in the earth's crust [ppm]	Safety level
Li	−3.040	19.2	3860	2061	3.40–3.82	20	1*☆
Na	−2.713	3.1	1166	1129	2.76–3.60	23 550	1*☆
Mg	−2.356	2.2	2206	3834	3.00–4.73	23 300	2*☆
Zn	−0.763	2.2	820	5855	4.04–4.30	70	5*☆
Al	−1.676	1.9	2980	8046	4.80	82 300	3*☆

passivation in aqueous electrolytes. The Zn metal can react with water to generate hydrogen gas, which would result in the local pH change of the electrolyte and thus promote the formation of zinc hydroxide sulfate (ZHS) or other Zn compounds in acidic/mild electrolytes, resulting in uneven distribution of electrolyte flux.^[16,17] The above-mentioned issues often cause the rapid failure of ZIB cells.^[10,18]

Approaches have therefore been explored to improve the stability and performance of the Zn anodes. Despite that there have already been several excellent reviews on the protection of Zn anodes,^[19–23] the novel materials and new surface/interface modification strategies continue to emerge and have not been covered by previous reviews. In this review, we aim to summarize the most recent progress in Zn anode protection with an emphasis on the surface and interface engineering. Specifically, we will discuss both the supports and protective coatings as well as their critical roles in inhibiting dendritic growth and corrosion of Zn anodes and the suppression of side reactions. The relationship between the issues, surface and interface engineering strategies, and the electrochemical performance (Figure 1) will be systematically discussed. Finally, we will provide an outlook for future directions of Zn anode design.

2. Main Challenges Facing Zn Anodes

The dendritic formation, corrosion, and passivation are the main obstacles in developing high-performance Zn anodes

(Figure 2A). The microstructure of the anode surface is rough and defective in some areas, resulting in fluctuant local Zn²⁺ ion concentrations under polarization. The Zn nucleation tends to proceed in the high Zn²⁺ concentration (i.e., high supersaturation) regions, and the Zn atoms will further deposit onto these nuclei, which eventually leads to the formation of “tips” and thus dendrites.^[24] The dendrite formation is largely affected by both the current density and capacity.^[1] Under large current densities, the Zn deposition is significantly accelerated, and the growth of dendrite is promoted. The charge would be continuously accumulated on the Zn tips (also known as the “tip effect”), creating a high electric field that further facilitates the growth of Zn dendrites, leading to the capacity fading and eventually a short circuit.^[26] Whereas when the current density is low, the Zn dendrite initiation time is delayed, and thus the growth rate decreases. In this case, the Zn dendrite growth has much smaller impacts on the battery lifespan as compared to that under high current conditions. It should be noted, however, the growth of the dendrite is a positive feedback process, and the dendrite can grow continuously. With the cumulative growth, the dendrites will eventually cause short circuit.

Corrosion and passivation of Zn anodes are also inevitable in aqueous electrolytes, which cause low utilization of the active metallic Zn, irreversible byproducts, and gas evolution.^[27] In mild aqueous electrolytes, the theoretical decomposition voltage of water is ≈1.23 V versus SHE (standard hydrogen electrode), and the standard electrochemical potential of Zn/Zn²⁺ can be expressed as:^[10]

$$E_0 = -0.763 + 0.059/2 \times \lg [\text{Zn}^{2+}] (\text{V}) \quad (2)$$

As shown in Figure 2B,^[20] the hydrogen evolution potential is related to the electrolyte pH. Therefore, the Zn anode is more violently corroded in acidic media because of the stronger hydrodynamic tendency of water toward the hydrogen evolution reaction (HER). The H₂ evolution leads to the accumulation of OH[−] ions on the Zn anode surface and thus promotes the formation of irreversible byproducts, such as ZnSO₄(OH)₆·xH₂O (ZHS).^[28] Whereas in alkaline electrolytes, Zn²⁺ ions tend to react with OH[−] and form insoluble byproducts (Zn(OH)₂, ZnO or other Zn composites, Figure 2B), which increase the battery's internal resistance and lead to rapid battery failure. Therefore, most alkaline Zn batteries with alkaline electrolytes are primary batteries since their rechargeability is still a big issue. This review will focus on the neutral or slight acidic aqueous electrolyte environment for Zn anode reactions.

It should be noted that the dendritic formation, corrosion, and passivation issues are mutually reinforced:^[29] the formation

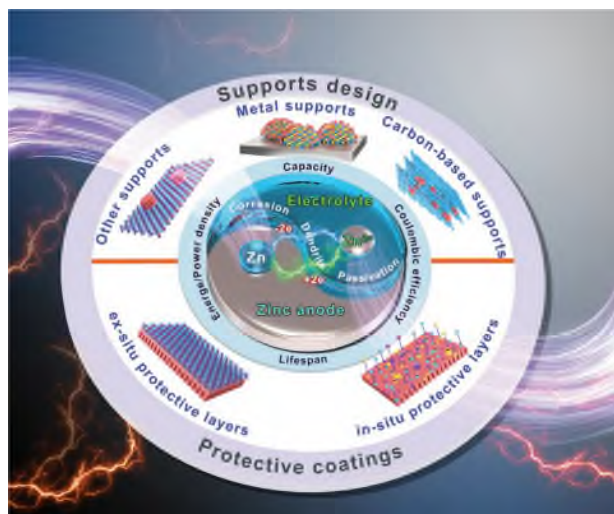


Figure 1. Design strategies for high-performance zinc anodes.

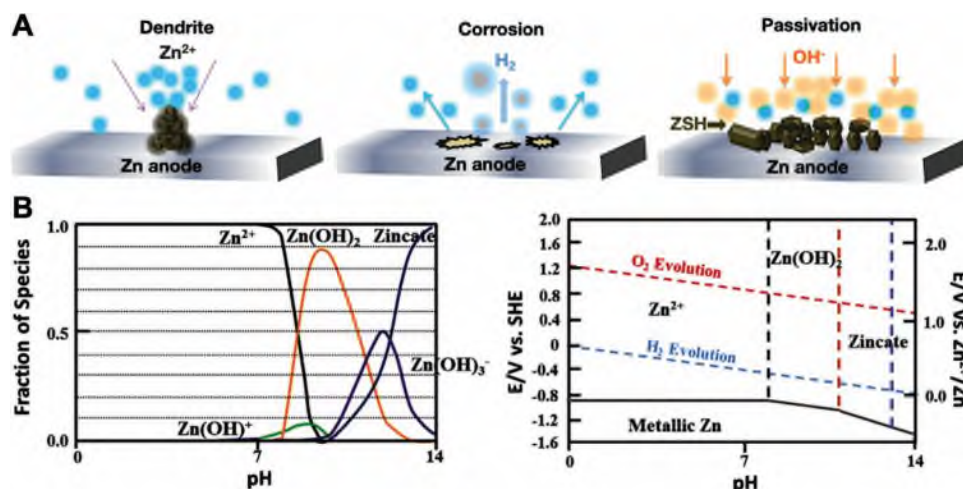


Figure 2. A) Dendrite growth, corrosion, and passivation phenomenon on Zn anode. B) Pourbaix diagram of a Zn/H₂O system in an aqueous electrolyte. Reproduced with permission.^[20] Copyright 2020, Elsevier.

of dendrites rapidly increases the surface area of anodes, which will promote the hydrogen evolution; conversely, corrosion and passivation make the Zn anode surface rough, which facilitates the formation of Zn dendrites. Besides, corrosion and passivation can make the chemistry of the anode surface different because corrosion cannot occur homogeneously. These will inevitably influence the surface properties. Intentionally etched Zn anodes can actually prolong the lifespan.^[30] In addition, electric field, current density, ionic conductivity, and electrolyte pH are also critical parameters that affect Zn plating/stripping. However, there is a limited possibility to control the reactions during the discharging/charging processes of bare anodes.

Fortunately, inspired by a myriad of research initiatives on Li metal batteries, many studies have demonstrated the benefits of surface and interface modification to alleviate the dendritic growth and side reactions. This can often be achieved by utilizing delicately designed supports or surface protective layers with desirable physicochemical properties. Generally, a support material for Zn anode should have properties of high surface area, excellent electronic conductivity, stable structure, and rich functional sites for Zn deposition. Whereas the surface protective layers should be able to inhibit dendritic growth and side reactions but allow the diffusion and deposition of Zn²⁺ ions. Below we will introduce the recent progress on the design and application of both the Zn supports and surface protective layers along with abundant examples.

3. Supports for Zn Anode

The Zn²⁺ ion stripping/plating processes are affected by the charge-transfer resistance, Zn²⁺ ion diffusion behavior, and redox reactions on the Zn anode surface.^[25,31] Different supports have been employed to optimize the electric field distribution and thus regulate the Zn deposition.^[32] Zn deposition on the heterogeneous supports needs to overcome the nucleation energy barrier, which is determined by the lattice parameters and the binding energy of the support materials with the Zn atom.^[19,33] A low nucleation barrier can be achieved on zinco-

philic supports or a sufficiently small lattice mismatch between the support and Zn. Several support materials including pure metals, alloys, polymers, carbons, and MXenes have been developed to improve the performance of Zn anode. In general, materials with delicate nanostructures, high electrochemical stability, large surface area, and low nucleation barrier are considered suitable supports for the stripping/plating of Zn. Next, we will introduce these supports with more details.

3.1. Carbons

Carbons, including carbon nanotubes (CNTs), graphite/graphene, carbon cloth (CC), and carbon belts, are popular supports for Zn anodes due to their low cost, light weight, low toxicity, large specific surface area, and easy functionalization.^[34–40] It is demonstrated that carbons' surface area and conductivity play critical roles in determining the performance. For example, the electric field distribution of 3D CNT scaffolds is more uniform than that of bare CC because of the larger specific area and smaller Zn nuclei size.^[41] The Zn/CNTs were found to possess a low nucleation overpotential and promote more homogeneous Zn²⁺ adsorption onto the electrode surface. The uniform electric field also avoids the “tip effect” caused by charge accumulation. However, the “dead” Zn on CNTs surface may promote the growth of Zn dendrites after long cycling. A sandwich-like anode structure (carbon fiber@Zn@carbon) was proposed to solve this problem (Figure 3A).^[42] Though it can enhance the lifespan, the utilization of active Zn is unsatisfactory. Since the Zn deposition behavior is highly related to the interactions between the Zn²⁺ ion and the carbon support, the performance can be further enhanced by tuning the intrinsic properties of the carbons. Kim et al. observed a strong orbital hybridization between Zn and the dangling bonds of the defective carbon support, which effectively suppresses the surface diffusion of Zn²⁺ ions and the consequent aggregation (Figure 3B).^[43] As a result, the Zn–Br flow batteries showed a long lifespan of over 5000 cycles even at a high current density/capacity of 100 mA cm⁻² and 20 mAh cm⁻². In addition, the

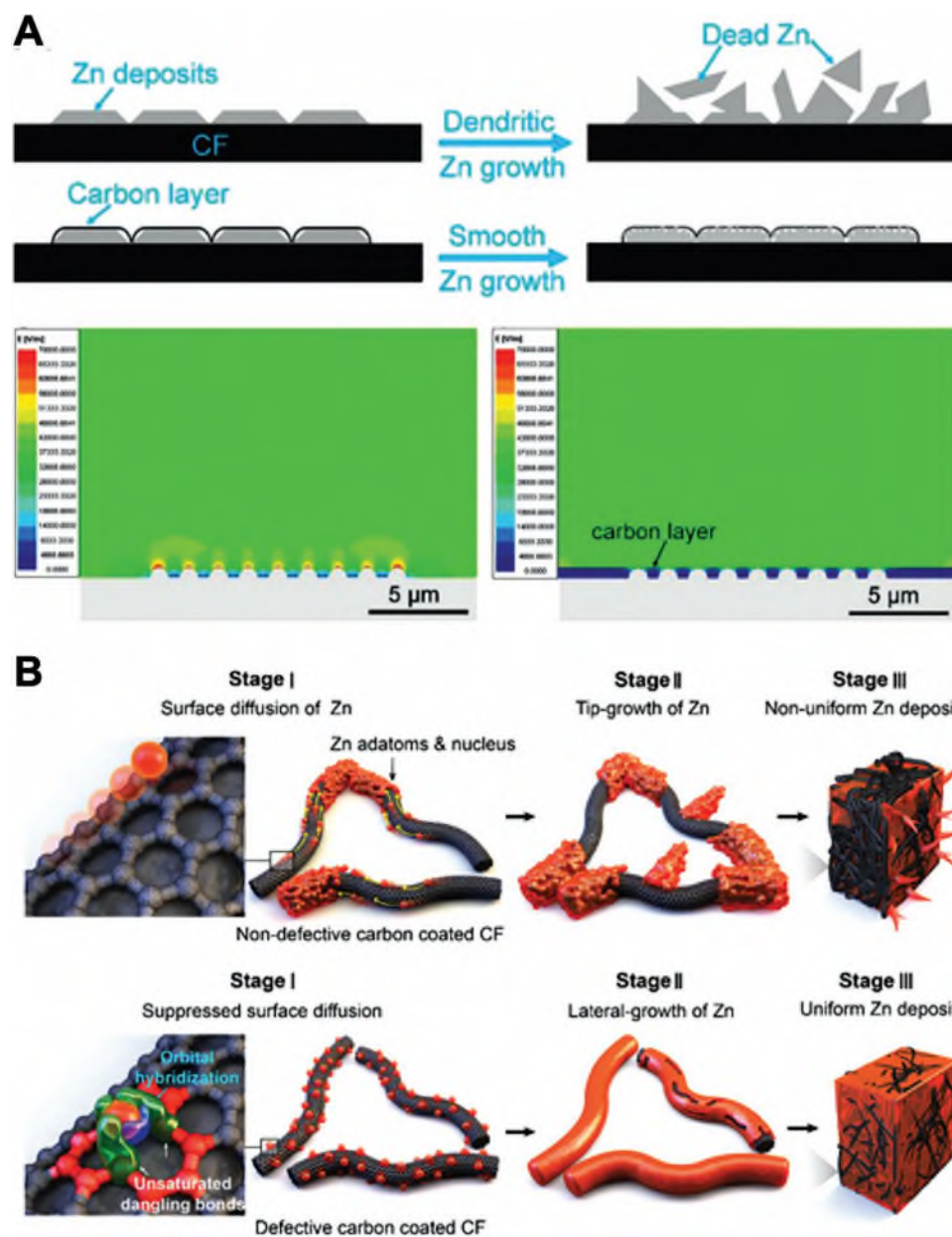


Figure 3. Carbon-based Zn anode supports. A) Schematic illustration showing the morphological evolution of CF@Zn and CF@Zn@C after long-term Zn plating/stripping cycles. Reproduced with permission.^[42] Copyright 2021, Wiley-VCH. B) Schematic illustration of Zn aggregation and subsequent Zn growth on the non-defective 3D CF and defective carbon layer-coated 3D CF. Reproduced with permission.^[43] Copyright 2020, The Royal Society of Chemistry.

carbon support-Zn interactions can be regulated by introducing functional groups. For instance, the carbon hosts with zincophilic sites (e.g., Zn–N bonds) can also achieve a homogenous Zn deposition.^[44]

Similarly, graphite and graphene with defective structure or heteroatom doping can serve as suitable supports for guiding Zn²⁺ ion nucleation.^[45,46] Zhang et al. demonstrated that the N and S co-doped 3D porous graphene framework provides more electroactive sites for Zn²⁺ ion deposition and thus leads to a significantly improved capacity and lifespan.^[47] Archer et al. constructed a graphene layer that has a minor lattice mismatch (≈7%) with Zn (002).^[48] The nucleation barrier for Zn²⁺ ion deposition

on the graphene layer is sufficiently small, and the Zn metal grows layer by layer with locked direction to maintain a minimal Gibbs free energy. They also revealed a strong metal–substrate interaction between the graphene-coated carbon fiber and Zn, which can effectively promote the uniform deposition of plate-like Zn with a minimized electron transport length scale.^[49] As a result, improved stability at high current density (60 mA cm^{−2}) was achieved. Although carbon supports have shown promising electrochemical performance, their mechanical strength is often unsatisfactory. The carbon framework failure often happens at high rates or long-time cycling. This will decrease the utilization of metallic Zn and create “dead Zn” areas that consequently pre-

vent the Zn^{2+} ions from continuous stripping/plating processes. In addition, when the Zn mass loading is high, the effectiveness of carbon supports dramatically decreases and the modified Zn anodes still suffer from Zn dendrites and side reactions. These are all the challenges that remain to be addressed in the future.

3.2. Metal Supports

Compared to carbons, metals often show higher conductivity and mechanical strength, which help to alleviate the degrada-

tion caused by structural and thermal failures. For example, 3D printed Ni-Zn anode with multi-channel lattice structures and the super-hydrophilic surface can effectively regulate the electric-field distribution and induce the uniform deposition of Zn without Zn dendrites (Figure 4A).^[50] The 3D structure can effectively enhance the lifespan of the Ni-Zn anode (Figure 4B). However, Ni itself electrocatalyzes water decomposition and produces hydrogen. Therefore, Ni supports may not be a good choice for ultra-long lifespan ZIBs. To avoid the water molecular decomposed by the electrocatalytic process, electrochemical inertia supports such as Cu are preferred. Cu

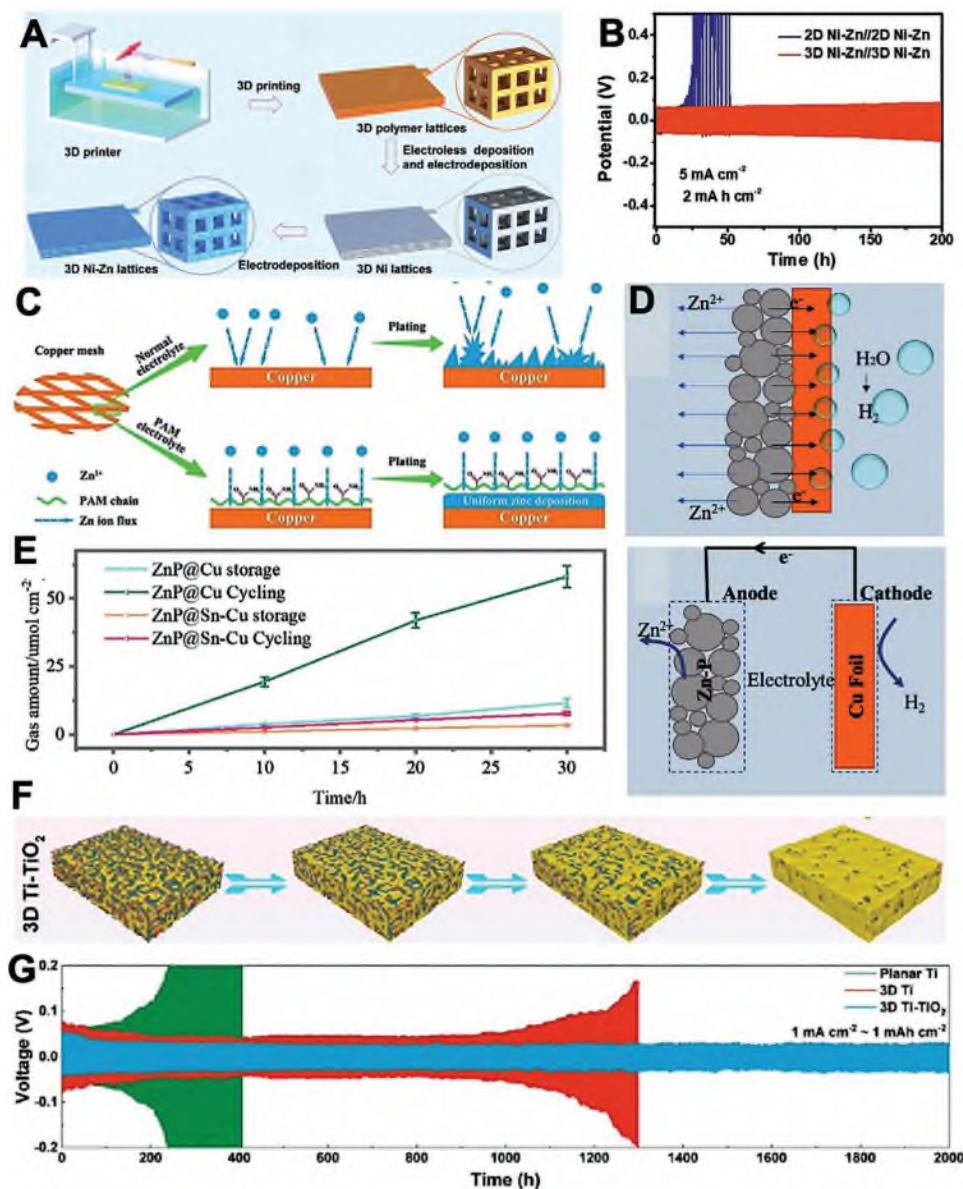


Figure 4. Metal supports for Zn anodes. A) Schematic illustration of the procedure for fabricating the 3D Ni-Zn support. B) Voltage profiles of 2D Ni-Zn and 3D Ni-Zn symmetric cells at 5 mA cm⁻², with 2 mA h cm⁻². Reproduced with permission.^[50] Copyright 2021, Wiley-VCH. C) The procedure of Zn²⁺ ion deposition on the copper mesh. Reproduced with permission.^[53] Copyright 2019, Wiley-VCH. D) Schematic of the galvanic corrosion between Cu@Zn-P and equivalent circuit of galvanic corrosion. E) Hydrogen production during Zn plating/stripping and aging. Reproduced with permission.^[54] Copyright 2021, Wiley-VCH. F) Zn deposition on Ti/TiO₂ 3D support. G) Voltage-time profile of symmetric Zn||Zn cells with different Zn metal anodes (Zn@Ti, Zn@3D Ti, and Zn@3D Ti-TiO₂) cycling at 1 mA cm⁻². Reproduced with permission.^[55] Copyright 2021, American Chemical Society.

foam and other porous Cu structures with large specific surface areas have shown to possess a low nucleation overpotential of Zn^{2+} ions.^[51,52] Although the 3D Cu skeletons can alleviate the Zn dendrite growth and electrocatalyze water decomposition, they can barely prevent the hydrogen evolution from Zn metal. Wang et al. therefore proposed a polyacrylamide (PAM) coated Cu mesh support to suppress the hydrogen evolution and achieved an enlarged voltage window (Figure 4C).^[53] Moreover, guided by the acyl group of PAM, the Zn^{2+} ions were evenly deposited onto the Cu mesh, simultaneously avoiding the growth of Zn dendrites. It should be noted that the HER process is difficult to completely diminish due to the galvanic corrosion between Cu and Zn (Figure 4D).^[54] To eliminate the side reactions, Zhi's group coated the Cu foil by Sn with a higher overpotential for hydrogen generation (Figure 4E). However, the Sn layer for Cu support may be depleted or covered by "dead Zn" after long cycling, which will be unable to inhibit the HER process. Therefore, the metal supports without galvanic corrosion with Zn and electric catalytic property are required. Ti foil is a stable metal support for ZIBs which has been widely used. For example, Qian's group constructed a 3D porous Ti with a spontaneous ultrathin zincophilic titanium dioxide (TiO_2) interfacial layer and continuous 3D structure (Figure 4F).^[55] The dendrite-free 3D Ti/Zn metal anode with a long lifespan of 2000 h at 1 mA cm^{-2} and 1 mAh cm^{-2} has been achieved due to the homogeneous nucleation, uniform electric field, and slight side reactions (Figure 4G), much superior to that of Ni or Cu supports modified Zn anodes.

In addition to external supports, the nanostructuring of Zn metal itself is also an effective way to modify the Zn surface and thus change the interfacial interactions with electrolytes. Wang et al. designed a 3D hierarchical porous Zn anode by organic etching of Zn metal, which enables preferential plating of Zn in the porous texture with suppressed dendrite growth.^[30] The kinetics of Zn^{2+} ion diffusion was promoted by the pore- and cavity-rich Zn foil surface. As a result, the lifespan of the 3D Zn anode is extended to 1500 h at $1.0 \text{ mA/mAh cm}^{-2}$. The surface properties of Zn can not only be modified by delicately designed nanostructures, but also are closely related to its crystallographic orientation.^[56,57] The preferred deposition of Zn (100) and (101) planes leads to the vertical growth of Zn with an angle of $\approx 70\text{--}90^\circ$, increasing the risk of Zn dendrite growth.^[58,59] On the other hand, the deposition of Zn (002) results in the lateral growth of Zn.^[60] The growth behavior of Zn deposit can be regulated by tuning the crystal facet of the Zn anode. Liang et al. demonstrated that the Zn (002) planes possess highest atomic packing density with even interfacial charge density and low surface free energy. Therefore, the Zn anode with more exposed (002) planes can effectively inhibit the dendrite growth.^[61] Meanwhile, Zn (002) planes with lower electrochemical active property further alleviate the by-product generation and corrosion behaviors on Zn anode.^[62,63] Recently, more (002) planes exposed metallic Zn anodes have been prepared by the plastic deformation^[64] and smelting method^[61] and achieved high Coulombic efficiency and long lifespan.

Compared to pure metal supports, zincophilic and chemically stable alloy seeds with non-galvanic corrosion, tunable elemental components, and low nucleation barrier have been considered as promising Zn anode supports, and examples

include zinc-silver (Zn-Ag), zinc-tellurium (Zn-Te), zinc-tin (Zn-Sn), zinc-copper (Zn-Cu), and zinc-aluminum (Zn-Al) alloys.^[65–71] Some metals such as Ag, Te, and Sn can "in situ" alloy with metallic Zn during the initial Zn plating and then serve as a support that further provides the Zn^{2+} ions deposit sites. For example, Xue et al. constructed a Ag nanoparticle-covered carbon cloth to realize reversible and dendrite-free Zn anodes for ZIBs (Figure 5A).^[67] During the Zn deposition process, zincophilic Ag seeds will alloy with Zn metal to form AgZn_3 alloy. The binding energies of Zn atom with Ag and AgZn_3 are -1.46 and -1.37 eV, respectively, which are lower than that of Zn atom with Zn (-0.68 eV) and carbon (-0.24 eV) substrates. Therefore, Zn atoms prefer to deposit onto the homogeneous Ag and AgZn_3 sites, which alleviates the dendritic growth during Zn deposition. The highly conductive Ag nanoparticles enhance the connection of carbon fibers, which decreases the amount of dead Zn during cycling. Finally, a near 100% Coulombic efficiency and a long lifespan of over 800 h at 2 mA cm^{-2} and 2 mAh cm^{-2} were realized (Figure 5B). Apart from the Zn-Ag alloy, Pu et al. revealed that Zn-Sn alloy is one of the effective supports for reducing side reactions during cycling (Figure 5C).^[66] The ratio of Sn in Zn-Sn alloy support directly affects the performance of the Zn anode. The Zn-Sn (001) alloy with a proper Sn content will enlarge the ΔG_{H^*} of surrounding adsorption sites and thus inhibit the production of H_2 at those sites, compared with pure Zn (001). Moreover, a proper Sn content can also lower the binding energy between Zn atom and Zn-Sn (100) surface, driving the flat Zn deposition on the alloy sites with a low nucleation barrier. On the other hand, a high Sn content will decrease the ΔG_{H^*} and thus lead to the hydrogen evolution. The SEM images illustrate that the surface of Zn-Sn-1 anode is smoother than that of the bare Zn and Zn-Sn-2 (with a higher Sn content) (Figure 5D). The cycling performance further confirms the addition of a proper content of Sn can enhance the stability of Zn anode (Figure 5E). Obviously, the "in situ" alloying can inhibit the growth of Zn dendrites and side reactions. However, the volumetric change of the alloy during the "in situ" alloying process may decrease the adhesion of the alloy and the current collector, and therefore lead to a performance decay.

An alternative way is to directly apply alloys as the supports. As for the direct fabrication of alloy supports, the accurate and stable nanostructure of alloy supports is required. Jiang et al. constructed lamella-nanostructured eutectic $\text{Zn}_{88}\text{Al}_{12}$ (at%) alloy as Zn anode (Figure 5F).^[70] The oxidative insulating layer of Al (i.e., Al_2O_3) allows the Zn^{2+} ions to selectively strip/plate from Zn sites of the Zn-Al alloy supports (Figure 5G). The superior oxidation-resistant capability of Zn-Al alloy endows low R_{ct} of ZIBs in the aqueous electrolyte. Finally, the lifespan of ZIBs was prolonged to 2000 h (Figure 5H). In short, the stable nanostructure and minimized galvanic corrosion are two critical factors for designing artificial alloy supports for high-performance Zn anodes.

3.3. Other Supports

Besides these two main categories (i.e., carbons and metals), a few other materials have also been proposed as the Zn anode

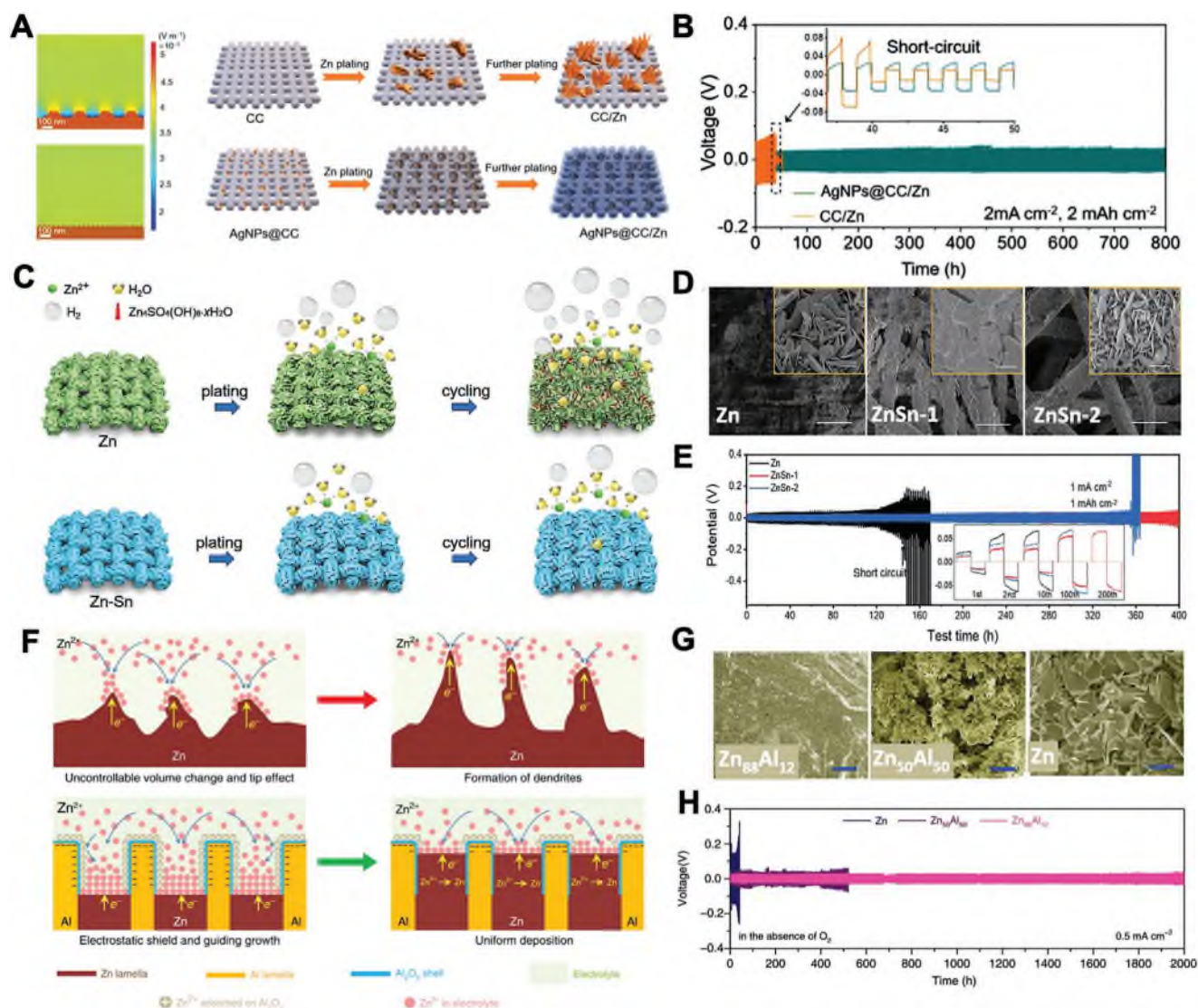


Figure 5. A) COMSOL simulation of the electric field distributions of CC/Zn and AgNPs@CC/Zn electrodes during the Zn deposition process. B) Voltage–time profiles of symmetric CC/Zn and AgNPs@CC/Zn cells at 2 mA/mAh cm^{−2}. Reproduced with permission.^[67] Copyright 2021, Wiley-VCH. C) Schematic illustration of the suppressed hydrogen evolution in Zn-Sn alloy electrodes. D) SEM images of different anodes after cycling for 120 h with the capacity of 5 mAh cm^{−2}. Scale bars: 100 and 5 μm (insets). E) Voltage–time profiles of symmetric Zn, ZnSn-1, and ZnSn-2 cells at 1 mA/mAh cm^{−2}. Reproduced with permission.^[66] Copyright 2021, Wiley-VCH. F) Illustration of the Zn deposition behavior on bare Zn and Zn-Al alloy anodes. G) SEM images of eutectic Zn₈₈Al₁₂ (Scale bars, 5 μm). H) Voltage–time profile of symmetric Zn, Zn₈₈Al₁₂, and Zn₅₀Al₅₀ cells at 0.5 mA cm^{−2}. Reproduced with permission.^[70] Copyright 2020, Springer Nature.

supports. For example, the 2D Ti₃C₂T_x MXene with elastic skeleton and big specific area can offer abundant active sites for Zn deposition, however, it suffers from the weak zincophilic ability. In this regard, hybridizing MXene with other materials with high zincophilic properties such as graphene is a smart strategy. Indeed, it has been demonstrated that the MXene/graphene can effectively inhibit the growth of Zn dendrites and the hydrogen evolution.^[72]

In general, an ideal support should have: 1) low nucleation barrier for Zn²⁺ ion plating; 2) high porosity or surface area; 3) stable and continuous skeleton; 4) no galvanic corrosion reaction with Zn. The various support materials and their corresponding electrochemical performances are summarized in Table 2.

4. Protective Layers for Zn Anodes

In ZIBs, the Zn anode directly contacts with aqueous electrolytes, which causes uncontrollable dendrite growth and corrosion.^[29] Interface modification by introducing surface protective coatings is an efficient strategy for improving the lifespan of Zn anodes. The artificial protective layers can be prepared by either ex situ or in situ approaches. The former is commonly fabricated by blade coating, electrostatic spinning, magnetron sputtering, atomic layer deposition (ALD), etc., which introduce a new phase on the Zn surface, whereas the latter involves the direct conversion of Zn metal to ZnF₂, ZnP, ZnSe, or other Zn-based compounds, which can be formed either by physical and

Table 2. Support materials for Zn anodes in ZIBs.

Type	Anode	Voltage hysteresis	Cycling performance	Ref.
Carbon	N, S co-doped graphene foams	58 mV (0.2 A g ⁻¹)	500 cycles (0.2 A g ⁻¹)	[47]
	Graphene/stainless steel	–	1000 cycles (40 mA cm ⁻²)	[73]
	Carbon cloth	–	5000 cycles (80 mA cm ⁻²)	[74]
	Flexible CNT	84 mV (5 mA cm ⁻²)	1000 cycles (20 mA cm ⁻²)	[41]
	Defective carbon	–	5000 cycles (100 mA cm ⁻²)	[43]
	Carbon fiber@Zn@Carbon	–	200 h (0.25 mA cm ⁻²)	[42]
Metal	Cu foam	65.2 mV (3 mA cm ⁻²)	300 h (2 mA cm ⁻²)	[52]
	3D porous Cu foil	≈40 mV (0.5 mA cm ⁻²)	350 h (0.5 mA cm ⁻²)	[51]
	3D Cu mesh	93.1 mV (2 mA cm ⁻²)	280 h (2 mA cm ⁻²)	[53]
	3D Ni	≈60 mV (5 mA cm ⁻²)	200 h (5 mA cm ⁻²)	[50]
	3D Ti	≈28 mV (1 mA cm ⁻²)	2000 h (1 mA cm ⁻²)	[55]
	Zn ₈₈ Al ₁₂	≈40 mV (0.5 mA cm ⁻²)	2000 h (0.5 mA cm ⁻²)	[70]
	3D Zn–Cu	≈20 mV (2 mA cm ⁻²)	300 h (2 mA cm ⁻²)	[71]
	Zn–Ni	–	–	[75]
	Zn–Te	–	–	[69]
	Zn–Ag	≈56 mV (2 mA cm ⁻²)	800 h (2 mA cm ⁻²)	[67]
Others	Zn–Sn	≈45 mV (1 mA cm ⁻²)	400 h (1 mA cm ⁻²)	[66]
	Ti ₃ C ₂ T _x MXene	75 mV (1 mA cm ⁻²)	300 h (1 mA cm ⁻²)	[76]
	MXene/graphene	–	1000 h (10 mA cm ⁻²)	[72]
	ZIF-8	–	1600 cycle (2.0 A g ⁻¹)	[77]

chemical treatments, or reacting with the electrolyte additives during the cycling. Next, we will discuss these two kinds of protective layers.

4.1. Ex Situ Formed Protective Layers

The growth of Zn dendrites and the side reactions are highly relative to the electric field distribution and Zn²⁺ ions diffusion behavior on the anode surface, as well as the nucleation barrier for the Zn²⁺ ions deposition.^[78,79] Fortunately, ex situ formed protective layers can modify the surface properties of bare Zn foil. Many protective coatings, including metal oxides, nitrides, polymers, metals, carbons, and MXenes have been investigated to modify the Zn anodes (Figure 6).

4.1.1. Metal Oxides

A series of metal oxides such as montmorillonite,^[80] BaTiO₃,^[81] ZnO,^[82] TiO₂,^[83] CaCO₃,^[84] ZrO₂,^[85] Al₂O₃,^[86] and kaolin,^[87] have been explored for protecting Zn anodes. The oxide coatings can avoid the direct contact of Zn with the aqueous electrolyte, therefore minimizing the side reaction. For example, Mai et al. demonstrated that the TiO₂ protective layer, even with a thickness of only 8 nm, can effectively prevent Zn from corrosion, and results in the enhanced electrochemical performance and improved Coulombic efficiency of Zn anodes.^[88] The Zn symmetric cell can cycle for ≈150 h at 1 mA cm⁻². Since most metal oxides are hydrophilic, which could enhance the inter-

action with water and thus promote the hydrogen evolution reaction, introducing additional hydrophobic compounds therefore become a popular strategy to inhibit the side reactions. For instance, Qie et al. constructed TiO₂ and polyvinylidene fluoride (PVDF) matrix as a coating layer for Zn anode.^[89] The PVDF layer blocks the water molecules on the anode surface, whereas nanosized TiO₂ layer guides the uniform Zn²⁺ stripping/plating. As a result, the Zn symmetric cell can cycle for over 2000 h at 0.885 mA cm⁻² with an ultralow Zn²⁺ ion deposition overpotential (<50 mV). An alternative strategy to modify the surface properties of the oxide coatings is to tune the specific crystal orientation. Wang et al. demonstrated that the TiO₂ (100) protective layers deliver a much better performance than that of TiO₂ (001) and (101) facets, which can be ascribed to their different binding energies with Zn (Figure 7A).^[83] The optimized Zn@TiO₂ symmetric cells can stably cycle for 460 h at 1 mA cm⁻² with a low voltage hysteresis (<40 mV).

In addition to TiO₂ coatings, other metal oxide layers such as CaCO₃,^[84] and ZrO₂,^[85] have also been investigated and achieved enhanced Zn anode stability. Interestingly, some oxide materials possess channels that allow the selective transport of Zn²⁺ ions, thus resulting in the homogeneous Zn deposition. For example, the Kaolin (Al₂(Si₂O₅)·(OH)₄) with sieve-element function (selective channel of Zn²⁺ ions) and uniform pore distribution (≈3.0 nm) can eliminate the dendrite, gas evolution, and enhance the capacity of ZIBs.^[87] The Kaolin (KL) layer contains abundant hydrogen-oxygen bonds, which are attributed to the silicon-oxygen tetrahedron and aluminum-oxygen octahedron sheets (Figure 7B). The special crystal structure endows the Kaolin layer with excellent Zn²⁺ ion affinity and low resistance

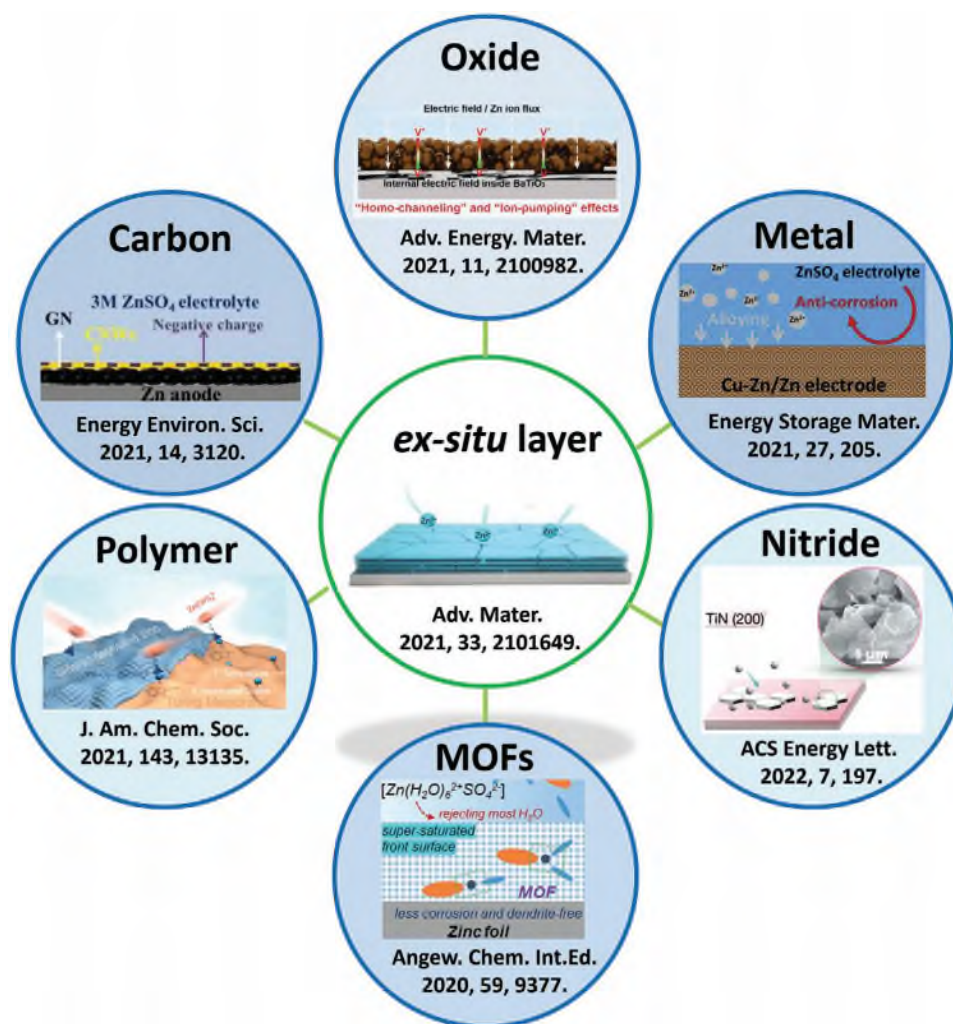


Figure 6. The main ex situ formed protective layers for Zn anodes. All images reproduced with permission.

for Zn nucleation. The Zn²⁺ diffusion through KL coating layer becomes stable after only 30 s, whereas the current of bare Zn keeps increasing beyond 200 s, indicating a long and frantic planar diffusion process (Figure 7C). The KL@Zn symmetric cell can cycle for 800 h at 4.4 mA cm⁻².

Although the metal oxide layers can enhance the lifespan of ZIBs, the oxide coatings may promote the side reactions because of the relatively high hydrophilicity. However, if the protective layer is hydrophobic, most of the Zn²⁺ ions may be repelled to the bulk electrolyte, which could possibly deteriorate the performance of ZIBs. Therefore, a proper hydrophilicity of oxide layer is necessary for long lifespan Zn anodes. In addition, since the oxides are typically semiconducting or even insulating, the Zn²⁺ ions would travel through the oxide layer and deposit onto the underneath Zn foil, which could break the connection between the oxide protective coating and Zn foil, therefore leading to the performance decay. Delicate nanostructuring or functionalization of the protective layers can modify the interfacial properties (e.g., the hydrophilicity) of oxide coatings and therefore regulate the Zn deposition behavior, resulting in an optimized stability of the Zn anodes.

4.1.2. MOF Coatings

MOFs (metal-organic frameworks) are widely used in energy-storage applications thanks to their metal ion nodes, functional linkers, and high specific surface area.^[90] MOFs typically show poor electronic conductivity due to the weak electron transfer through coordination bonds between the metal core and organic linkers,^[91] which is a disadvantage as electrode materials but could be a useful merit when used as surface protective layers. MOF layer can be combined with Zn anode by hydrothermal, liquid phase diffusion, and other preparation methods. Coating MOF layer on Zn anode can alleviate the charge accumulation at the Zn anode surface and provide enough activity sites for Zn²⁺ ion deposition. In addition, the wettability between the electrolyte and Zn anode is very important for Zn²⁺ ion diffusion. Pan et al.^[92] verified that the hydrophilic surface of Zn anode can enhance the Zn²⁺ ion diffusion in the mild aqueous electrolytes. They mixed MOF with polyvinylidene fluoride (MOF-PVDF), then covered Zn anode with MOF-PVDF coating to enhance the hydrophilicity of the Zn anode surface. The contact angle of the UIO-66 MOF modified Zn anode (53.4°) is significantly

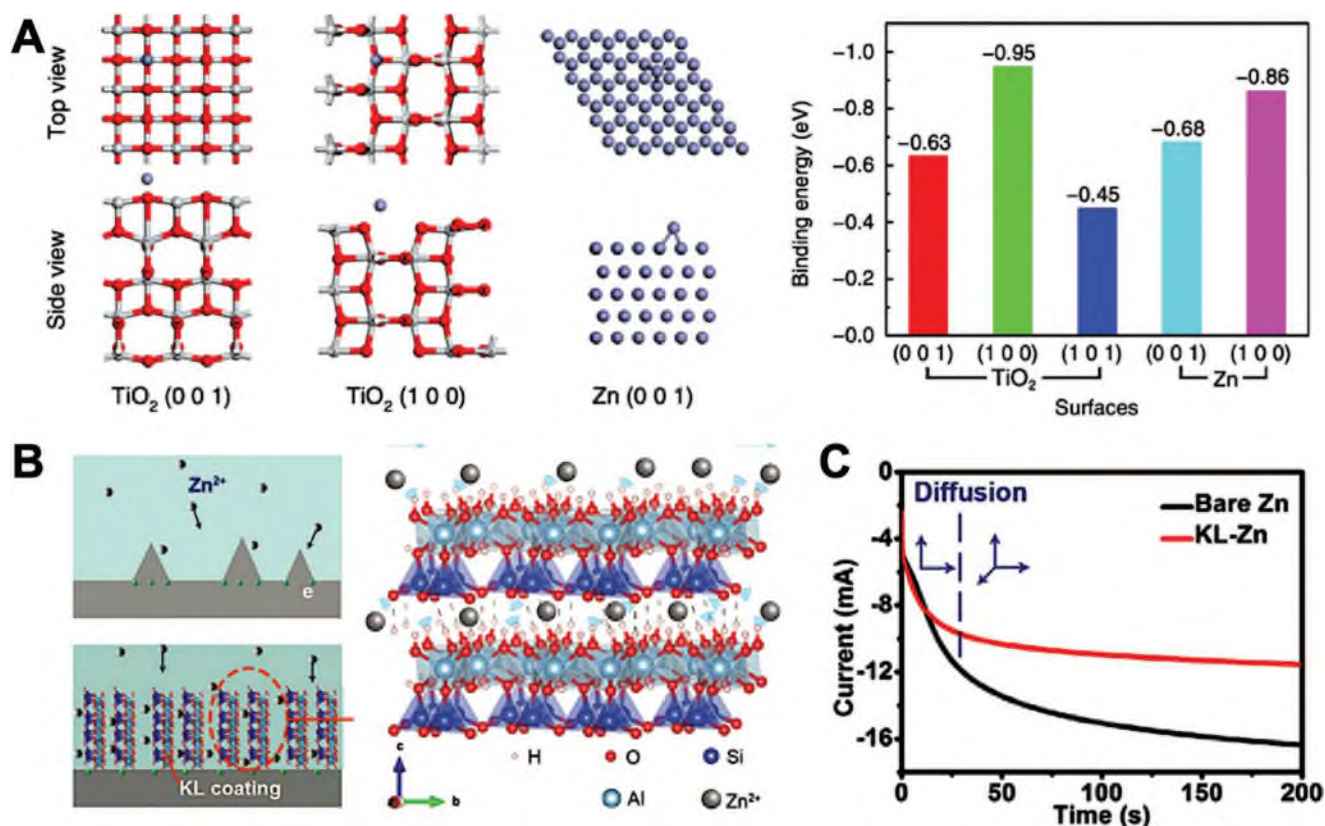


Figure 7. A) Calculated binding energies of Zn atom with different TiO₂ facets. Reproduced with permission.^[83] Copyright 2020, Springer Nature. B) Schematic illustrations of the morphology of Zn and KL-Zn anodes during Zn²⁺ ion deposition process and C) chronoamperograms (CAs) of bare Zn and KL-Zn at a -200 mV overpotential. Reproduced with permission.^[87] Copyright 2020, Wiley-VCH.

lower than the bare Zn anode (88.3°). The zincophilic interface reduced the charge transfer resistance and Zn²⁺ ion deposition overpotential from 92 to 41 mV at 2 mA cm⁻². Low resistance and uniform electrolyte distribution have been achieved due to the zincophilic surface, resulting in dendrite-free and stable Zn anode. Zhou et al. further investigated the solvation structure of electrolytes in MOF ZIF-7 pore to understand why the MOF layer inhibits dendrite growth and side reactions.^[93] The microporous MOF channels do not allow the large-radius solvated ions ([Zn²⁺(H₂O)₆SO₄²⁻] or [Zn²⁺(H₂O)₅OSO₃²⁻]) to pass (Figure 8A). Only small solvated ion H₂O-Zn²⁺·OSO₃²⁻ can successfully move through the MOF channels (Figure 8B). The result can be confirmed by Raman spectra (Figure 8C). Compared with bulk electrolyte, the Raman peak of ν-SO₄²⁻ in MOF channels shifted from 983–985 to 992 cm⁻¹, which means that Zn²⁺ ion is constrained with anions to form [ZnSO₄²⁻] ions. At the same time, the intensity of -OH stretching vibration is suppressed, indicating that a small amount of water is trapped in MOF pores. In order to investigate the diffusion mechanism of Zn²⁺ in the MOF layer, Xu et al. used ZIF-8 as the ion modulation layer to tune the ion diffusion behavior of Zn²⁺. They found that the ZIF-8 layers are critical for homogenizing Zn²⁺ ion flux distribution and decreasing the energy barrier for metal nucleation on the surface of the ZIF-8@Zn electrode (Figure 8D).^[94] Therefore, the ZIF-8 protective coating on the Zn anode avoids an uneven distribution of the electric field and thus inhibits the formation of protuberances/dendrites.

Obviously, modifying Zn anode with MOFs is an effective strategy for obtaining high-performance Zn anode. The big family of MOFs brings about huge opportunity as the properties of MOFs can be tailored by tuning the linkers and metal compounds, and there are only a few MOFs that have been explored for Zn anode protective layers. However, there are still disadvantages of MOFs layers which may also induce harmful impurities to the ZIBs's system. Importantly, the weak strength of the MOFs layer and poor adhesion between coating and substrate will deteriorate the homogeneous ion distribution. Mechanical stability of MOFs' layers is required for long-lifespan Zn anodes.

4.1.3. Metal Coatings

Metal nanoparticles with small size, high conductivity, and excellent chemical/physical stability can be used as the crystal seeds for Zn²⁺ ions nucleation and alleviate the charge accumulation on the Zn anode surface. Au nanoparticles (NA) have been sputtered to cover the Zn surface (Figure 9A),^[95] which offers an even local electric field and abundant sites for Zn²⁺ ion deposition. The high-curvature "tip" with lots of electrons would cause the Zn²⁺ ions to accumulate on the anode surface. The initial deposition overpotential of NA-Zn (342 mV) is higher than the bare Zn (137 mV) due to the lower nucleation barrier for Zn²⁺ ions on NA. The cyclability of the NA-Zn anode is better than

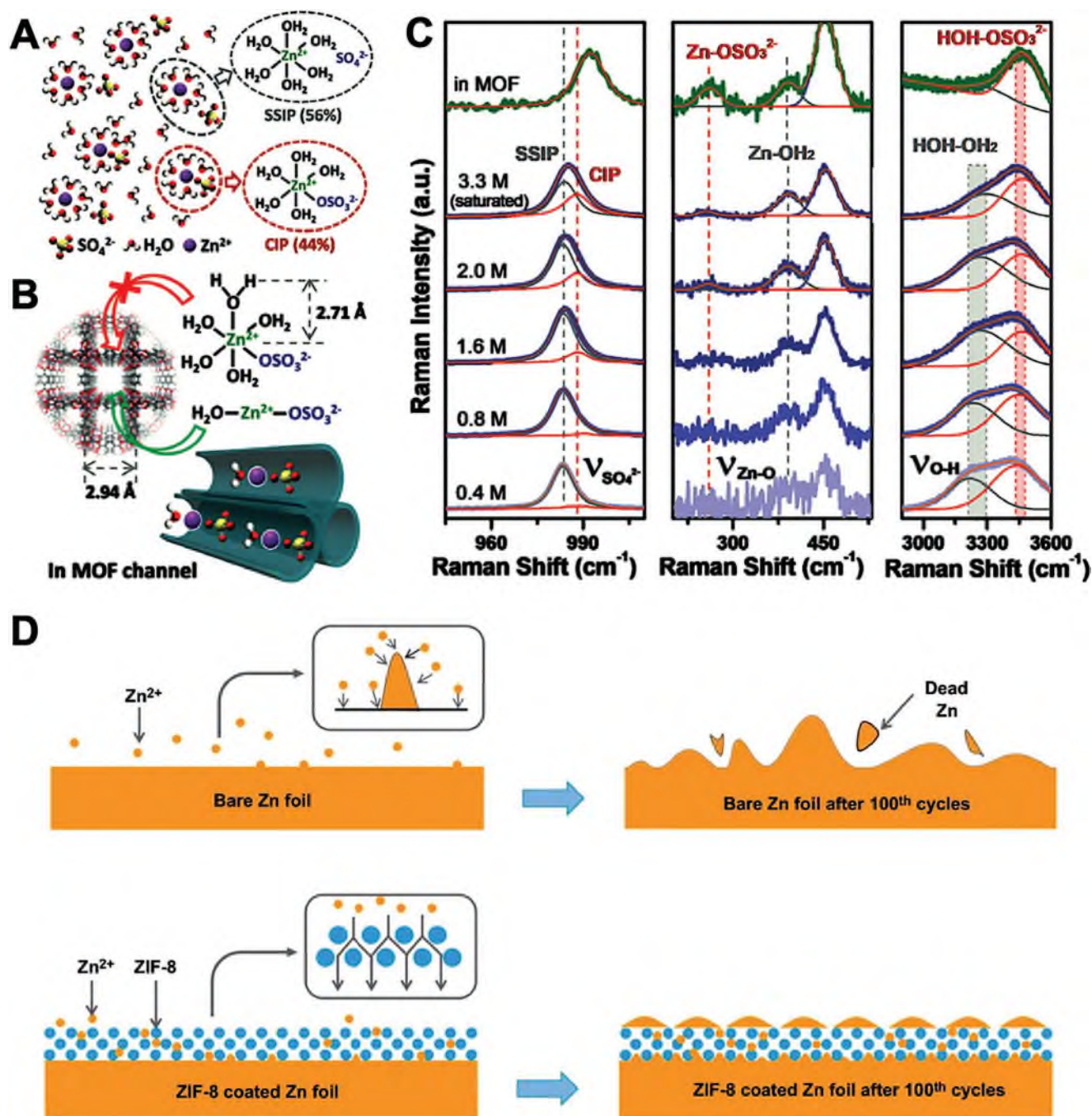


Figure 8. A) Two solvation structures in saturated (3.3 M) ZnSO_4 electrolyte and B) Radius of two solvation ions and channels of MOF. C) Raman patterns for bare and MOFs modified Zn anode reaction. Reproduced with permission.^[93] Copyright 2020, Wiley-VCH. D) Schematic illustration for morphology evolution of the bare Zn and ZIF-8@Zn anodes during stripping/plating processes. Reproduced with permission.^[94] Copyright 2020, Springer Nature.

the bare Zn anode because Au particles can also act as the support materials for Zn^{2+} ion deposition (Figure 9B). The NA-Zn anode surface is smooth after several hundred cycles. However, due to the high overpotential for Zn^{2+} ion deposition, the hydrogen evolution, and side reactions cannot be alleviated. A passivation layer may appear between the Au particle and Zn anode surface if the modified anode works in alkaline electro-

lytes. Therefore, it is urgent to design an anti-corrosion metal coating for Zn anode. Kang et al. constructed an In coating on the Zn anode to enhance the corrosion resistance of Zn metal (Figure 9C).^[96] Compared to the bare Zn anode, there are few $\text{Zn}_4\text{SO}_4(\text{OH})_6 \cdot 3\text{H}_2\text{O}$ on the In@Zn anode. According to the theoretical calculations, the In metal possesses higher adsorption energy for the Zn atom than the Zn substrate, which

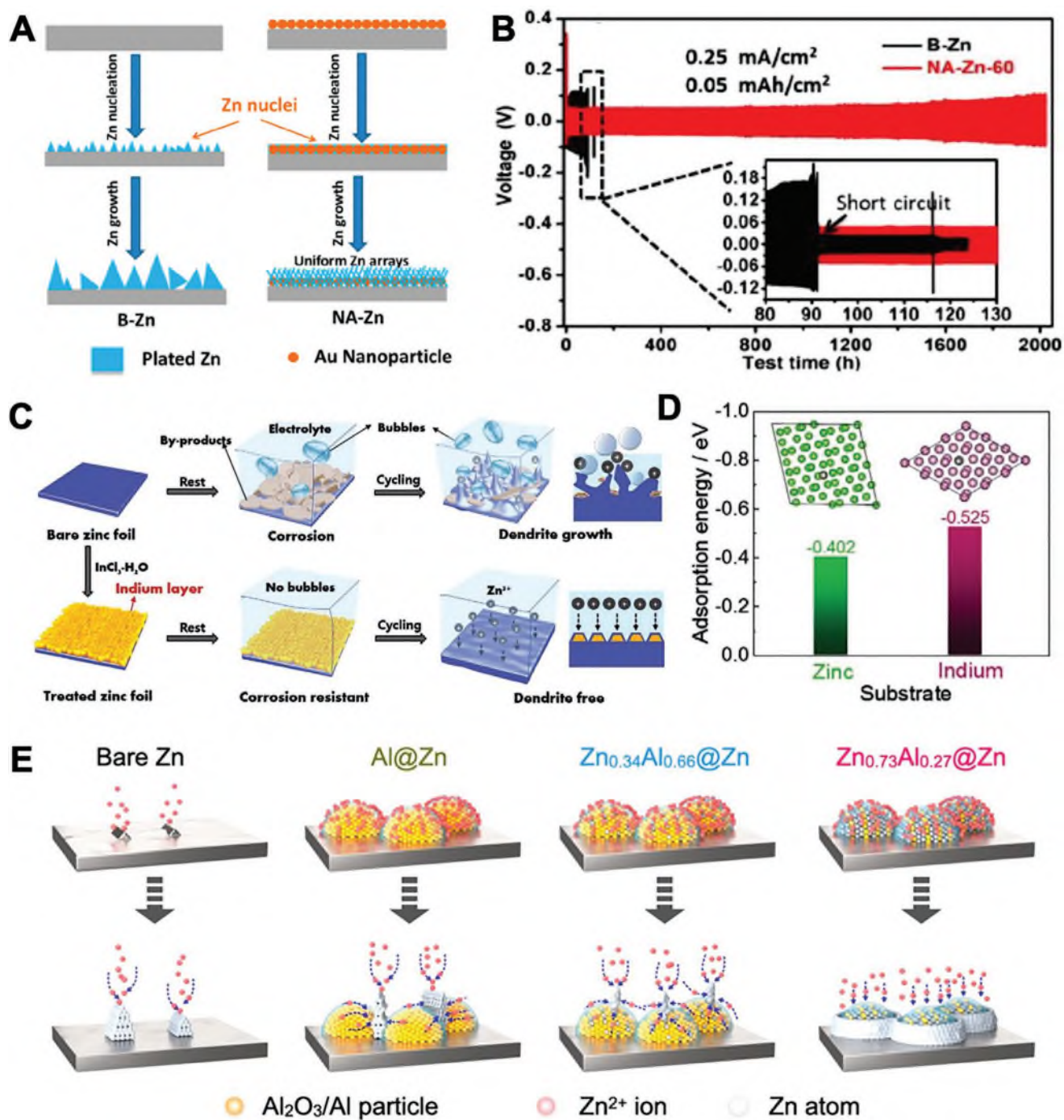


Figure 9. A) Zn stripping/plating process on a bare Zn (B-Zn) and NA-Zn. B) long-term discharge/charge profiles of Zn|Zn symmetrical cells with B-Zn (black lines) or NA-Zn electrodes (0.25 mA cm⁻² with 0.05 mA h cm⁻²). Reproduced with permission.^[95] Copyright 2019, American Chemical Society. C) Schematics of preparing Zn-In coating and the behavior of bare Zn and Zn|In anodes in an aqueous ZnSO₄ electrolyte. D) Adsorption energy of a Zn atom on zinc and indium substrates. Reproduced with permission.^[96] Copyright 2020, Wiley-VCH. E) Schematic illustration of Zn deposition on different Zn electrodes. Reproduced with permission.^[97] Copyright 2022, American Chemical Society.

indicates that the Zn²⁺ ions prefer to deposit on the In metal (Figure 9D). Finally, the long lifespan of In@Zn anode was demonstrated by cycling for 1495 h at 0.2 mA cm⁻² with ≈50 mV voltage hysteresis. In addition to the above-mentioned materials, our group found that the Zn deposition behavior can also be regulated by Al-based alloy protective layers (Figure 9E).^[97]

The Al can form a surface insulating Al₂O₃ layer and by manipulating the Al content of Zn–Al alloy films, they were able to control the electrostatic shielding strength, therefore realizing a long lifespan of Zn anodes of up to 3000 h at a practical operating condition of 1.0 mA/mAh cm⁻². In addition, the concept can be extended to other Al-based systems such as Ti–Al alloy

and achieve enhanced stability of Zn anodes, demonstrating the generality and efficacy of the strategy.

4.1.4. Carbon Coatings

Carbons with different functional groups possess different adsorption and binding energies with Zn^{2+} ions. And the diverse architectures of carbon-based coatings can be achieved by tuning processing methods.^[98] Reduced graphene oxides (rGO) coated Zn surface was confirmed to be capable of inhibiting dendrite growth.^[99] Later, other graphene-related materials such as graphene spheres, graphene cages, graphene vertical sheets etc., have been developed for Zn anode coating.^[100] For example, Dai et al. produced highly porous graphene-like carbon film (GCF) coated Zn anode and MnO_2 cathode.^[101] The ZIBs achieved $381.8 \text{ mA h g}^{-1}$ at 100 mA g^{-1} and a reversible capacity of $188.0 \text{ mA h g}^{-1}$ after 1000 cycles at 1000 mA g^{-1} . Zhi et al. used hydrogen-substituted graphdiyne (HsGDY) with sub-angstrom level ion tunnels and robust chemical stability as an artificial interface layer to protect the Zn anode.^[102] The HsGDY coating can guide the Zn^{2+} ion diffusion along the HsGDY–Zn interface to form uniform electric fields and avoid the dendrite growth during the charge/discharge process (Figure 10A). The symmetric cell can cycle for >2400 h at $0.5\text{--}2 \text{ mA cm}^{-2}$ with $\approx 50 \text{ mV}$ voltage hysteresis. Proper thickness of the modified carbon layer can not only enhance the Zn^{2+} ion diffusion kinetics but also inhibit the Zn anode corrosion.^[103] In addition, heteroatom doping is also an effective strategy to introduce zincophilic sites for Zn deposition. Chen et al. demonstrated that an ultrathin nitrogen (N)-doped graphene oxide (NGO) layer can greatly enhance the stability of Zn anodes (Figure 10B).^[104] The directional deposition of Zn (002) planes was achieved thanks to the parallel graphene layer and beneficial zincophilic-traits of N-doped groups (Figure 10C). As a result, uniform Zn deposition at high current density with greatly suppressed side reactions and Zn dendrites growth was achieved (Figure 10D).

4.1.5. Polymer Coatings

Polymer coatings are promising alternatives for protecting Zn anode due to their flexibility and porous skeleton, adjustable polar groups, and eco-friendless. The basic design principles of polymer coatings for Zn anode are the following. First, the coating should be ionically conductive but electronically insulating. Second, the polymer coatings should be dense and insoluble in aqueous electrolyte. Third, the protective layer should be hydrophilic for guiding ion diffusion in the coating. Last, it should possess strong adhesion to Zn metal surface and good mechanical properties.^[105,106] Many different kinds of polymers have been applied as protective coatings for Zn anode. Theoretical analysis shows that the polymer coating can inhibit the Zn dendrite growth in aqueous electrolytes by utilizing the mechanical suppression effect from the porous skeleton and the fast ion diffusion kinetics.^[107] Polyacrylamide (PAM)/polyvinylpyrrolidone (PVP) coated Zn anode was explored by Li et al.^[108] The PAM with large molecule weight guarantees the strong adhesion

of the coating to the Zn anode. And the PVP contains a stable pendant five-membered ring. Importantly, the PAM/PVP coating provides abundant polar groups ($\text{C}=\text{O}$ and N-H bonds), which can act as adsorption sites. Thus, the polymer layer can guide Zn^{2+} ions to uniformly diffuse along the polymer chains to Zn surface and also as an electrostatic shield to eliminate the charge accumulation at the Zn cusps. As a result, the cycling performance of ZIBs was improved. The viscoelastic hydrophilic polyvinyl butyral (PVB) can also reduce the interfacial free energy of Zn anode and electrolyte to ensure homogeneous plating and nucleation (Figure 11A).^[106] The ionic conductivity of the electrolyte is another critical factor that affects the performance of Zn anode. The zinc perfluorinated sulfonic acid membrane (ZPSAM) with a high ionic conductivity ($1.7 \times 10^{-3} \text{ S cm}^{-1}$) and hydrophilic properties was employed to increase the mass transport kinetics of Zn^{2+} ions.^[109] Significantly, the ZPSAM layer can provide suitable channels for Zn^{2+} ion diffusion from the electrolyte to Zn anode surface. In contrast, Zn^{2+} ions on bare Zn anode prefer to accumulate in some areas to form dendrites (Figure 11B). Cui et al. revealed that free water/ O^{2-} can induce corrosion and passivation.^[105] Polyamide (PA) coating could block free water molecules, increasing the nucleation barrier and restrict the diffusion of the Zn^{2+} ions with a 2D pathway.^[105] In addition to the free water/ O^{2-} , the SO_4^{2-} ions are critical sources for forming side products ($\text{Zn}_4\text{SO}_4(\text{OH})_6 \cdot x\text{H}_2\text{O}$), which is insulating and insoluble. Nafion-Zn-X coating is an organic-inorganic hybrid interfacial protection layer, which can effectively block the free water molecule and SO_4^{2-} ions because of its negatively charged framework and small pore size (Figure 11C).^[110] According to the DFT calculations, the desolvation energies of Zn^{2+} ion (-1.7 to -2.9 eV per atom) with different amounts of H_2O molecules are much lower than free Zn^{2+} ions in water (-14.9 eV per atom), which implies faster transfer kinetics of Zn^{2+} ions in the Nafion-Zn-X film.

In short, mechanically stable polymer coatings such as PAM/PVP, PA, PVB, ZPSAM, and Nafion-Zn-X with high hydrophilicity and specific functional groups have been explored to guide Zn^{2+} ion deposition and prevent the free water molecule and SO_4^{2-} ions from attacking the Zn anode, which can effectively inhibit the Zn dendrite growth and corrosion.

In addition to the above-mentioned materials, some of the catalytically inert metal nitrides have also shown the capability as the surface protective layers for Zn anodes.^[111,112] For example, Liang et al. demonstrated that TiN coatings with specific orientation can effectively suppress the Zn dendritic growth as well as the side reaction.^[113] More interestingly, they showed that the TiN (200) can induce a lateral growth of byproduct, whereas TiN (111) results in a vertical growth, which is associated with the surface atomic arrangements of the TiN layer. As a result, a long lifespan of over 2000 h at 1 mA/mAh cm^{-2} was achieved. The various ex situ coating materials and their corresponding electrochemical performance are summarized in Table 3.

4.2. In Situ Formed Protective Layers

Compared to the ex situ formed protective layers, the in situ formed layers do not require additional binders and often possess stronger adhesion. To date, several kinds of in situ formed

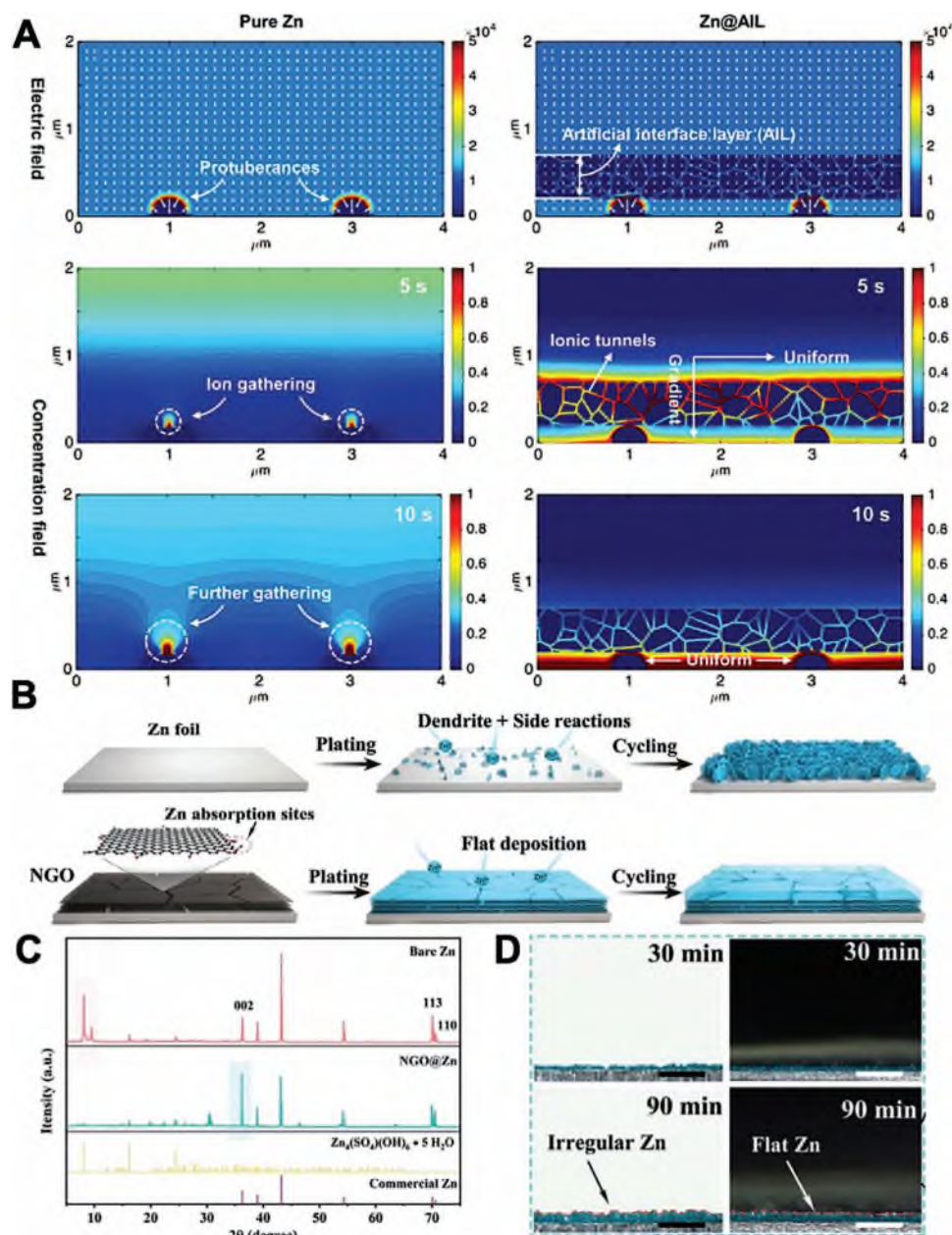


Figure 10. A) Dual-field simulations uncover the redistribution of Zn^{2+} ion concentration field achieved by modified layer. Reproduced with permission.^[102] Copyright 2020, Wiley-VCH. B) Schematic illustration of Zn deposition on bare Zn and NGO@Zn electrodes. C) XRD patterns of bare Zn and NGO@Zn anodes after electroplating, respectively. D) In situ optical microscopy visualization of Zn plating on bare Zn (left) and NGO@Zn electrodes (right) at 5 mA cm^{-2} . Scale bar: $100 \mu\text{m}$. Reproduced with permission.^[104] Copyright 2021, Wiley-VCH.

protective layers, such as ZIF-8,^[114] carbon,^[115] zinc phosphate,^[116] ZnF_2 ,^[117–119] ZnP ,^[120] ZnSe ,^[121–123] Zn /indium hydroxide sulfate,^[124] AgZn_3 ,^[125] and polydopamine,^[126] have been reported. These layers are generally in situ formed by electrochemical synthesis, thermal calcination, chemical treatment and other strategies.

4.2.1. Electrochemically Generated Layers

Some Zn-containing surface protective layers can be synthesized by electrochemically reacting the Zn metal with other

chemicals. The thin films formed by such strategy often exhibit 3D porous surface and functional sites that benefit the uniform Zn^{2+} flux. Li et al. fabricated a 3D interconnected ZnF_2 matrix on Zn anode using an electrochemical treatment method (Figure 12A).^[117] The ZnF_2 @Zn electrode can efficiently redistribute the Zn^{2+} ion flux and significantly reduce the desolvation active energy, leading to the stable and facile Zn deposition kinetics.^[117] Besides, the ZnP protective layer also can be electrodeposited onto the Zn anode using specific solution.^[120] The phosphorus atoms in the coating layer were found to fasten ion transfer and reduce the electrochemical activation energy

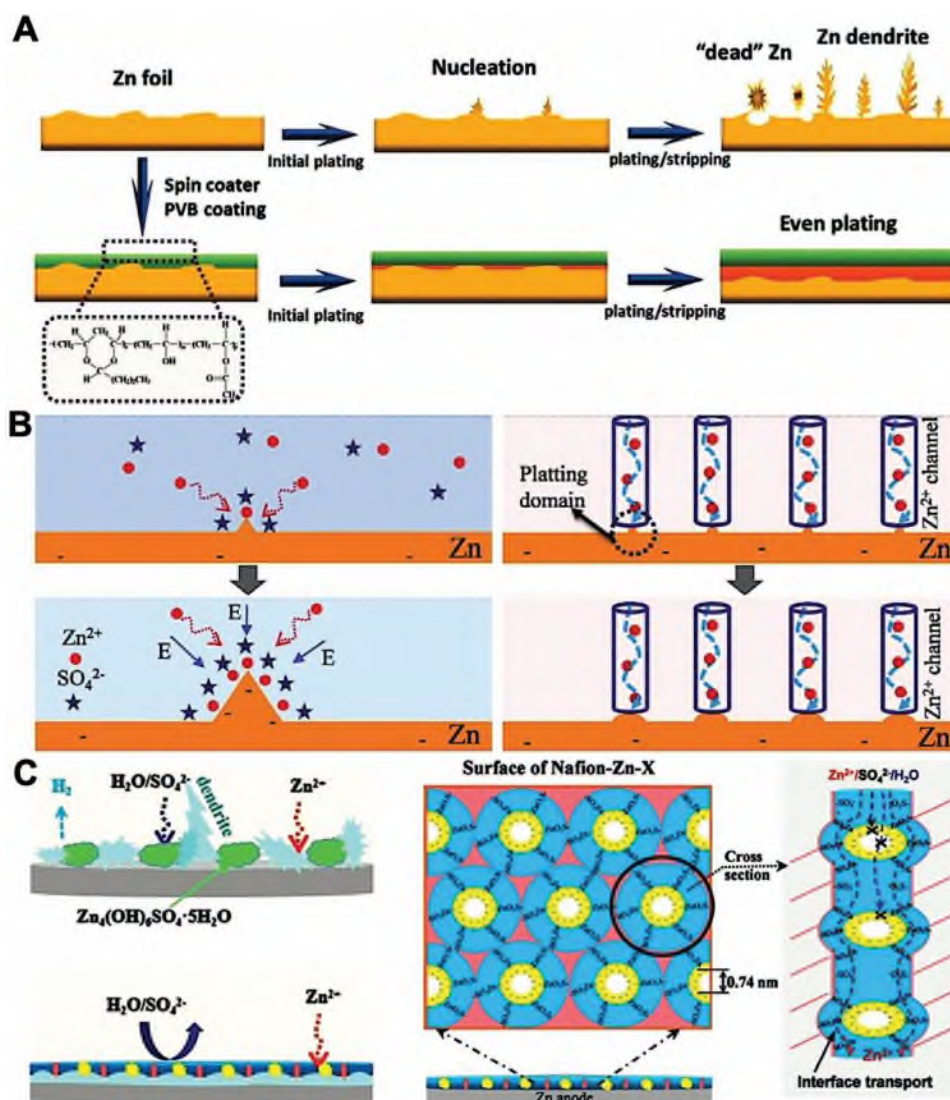


Figure 11. A) Zn anode morphology for bare Zn–Zn cell and the PVB@Zn–PVB@Zn ZIBs during stripping/plating. Reproduced with permission.^[106] Copyright 2020, Wiley-VCH. B) Zn plating with ZnSO₄ electrolyte and ZPSAM electrolyte. Reproduced with permission.^[109] Copyright 2020, Elsevier. C) Zn²⁺ deposition and transportation on Nafion–Zn–X coated Zn anode surface. Reproduced with permission.^[110] Copyright 2020, Wiley-VCH.

during Zn stripping/plating processes (Figure 12B).^[120] In addition, a lower energy barrier of Zn²⁺ ions transferring into the coating can be attained due to the additional phosphorus. Although these in situ formed protective layers can enhance the lifespan of Zn anodes, they might be destroyed or dissolved upon battery operation due to the lack of self-healing ability. Alternatively, in situ generation of protective layers during cycling is proposed. For example, a multifunctional polydopamine layer could be generated in situ on the Zn anode surface by using 1 M Zn(CF₃SO₃)₂ electrolyte containing dopamine additive (Figure 12C).^[126] The thin polydopamine layer (≈ 40 nm) shows a high Zn²⁺ ionic conductivity and outstanding hydrophilicity, which not only regulates the homogeneous distribution of Zn²⁺ ion flux, but also suppresses the hydrogen evolution. The good adhesion ensures the dense and tight binding between the protective layer and Zn surface. In addition, the in situ deposited layer often exhibits self-repairing ability, there-

fore enabling prolonged lifespan of Zn anodes (Figure 12D). However, the thin layer may be covered by the dead Zn after long cycling, which would cause the irreversible consumption of additives and eventually lose the functionality.

4.2.2. Thermally Generated Layers

Thermal calcination has also been employed to prepare ZnF₂, ZnSe, carbons, and other layers by using different gases (such as NH₃, H₂/Ar, O₂, and so on) under low temperature (<250 °C). For instance, the ZnSe protective layer was prepared by thermal calcination of Zn under H₂/Ar atmosphere (Figure 13A).^[122] The ZnSe layer can not only guide the growth of Zn along the (002) direction at the initial stage of stripping/plating cycles, thereby inhibiting the formation of Zn dendrites, but also suppress the side reaction (Figure 13B).

Table 3. Advances of different coating materials for ZIBs.

Type	Anode	Working Mechanism	Ionic conductivity	Cycle performance	Ref.
Ex situ formation layer	3D nano porous ZnO	Low activation energy	–	500 h (5 mA cm ⁻²)	[82]
	Faceted TiO ₂	Low zinc affinity	–	450 h (1 mA cm ⁻²)	[83]
	ALD TiO ₂	Large active surface area	–	1000 cycles (3 mA cm ⁻²)	[88]
	TiO ₂ /PVDF	Blocking H ₂ O/O ₂	–	2000 h (0.885 mA cm ⁻²)	[89]
	Kaolin	Selective Zn ²⁺ diffusion channel	–	800 h (4.4 mA cm ⁻²)	[87]
	Nano-CaCO ₃	Selective Zn ²⁺ diffusion channel	–	>800 h (0.25 mA cm ⁻²)	[84]
	ZrO ₂	Blocking H ₂ O	–	>3800 h (0.25 mA cm ⁻²)	[85]
	Sc ₂ O ₃	Blocking H ₂ O	–	>250 h (0.5 mA cm ⁻²)	[130]
	BaTiO ₃	self-accelerate ion migration	1.428 mS cm ⁻¹ (5 μm)	>4000 h (1.0 mA cm ⁻²)	[131]
	Montmorillonite	High ionic conductivity	3.9 mS cm ⁻¹ (1.5–50 μm)	>1000 h (1.0 mA cm ⁻²)	[80]
	ZIF-8	Uniform Zn ²⁺ distribution	–	>160 h (0.25 mA cm ⁻²)	[94]
	ZIF-7	Super-saturated electrolyte layer	–	2000 h (0.5 mA cm ⁻²)	[93]
	Au-nanoparticle	Zn nuclei seeds	–	2000 h (0.25 mA cm ⁻²)	[95]
	Metallic indium	High adsorption energy	–	1500 h (0.2 mA cm ⁻²)	[96]
	Ag	Zn nuclei seeds	–	2500 h (0.25 mA cm ⁻²)	[125]
	Cellulose nanowhisker-graphene	High ionic conductivity, anti-corrosion	29.2 mS cm ⁻¹ (52 μm)	5500 h (0.25 mA cm ⁻²)	[132]
	Mesoporous hollow carbon spheres	Large active surface area ordered nanochannels	–	500 h (1 mA cm ⁻²)	[133]
	Hydrogen-substituted graphdiyne	Sub-angstrom level ion tunnels, H atom	–	>2400 h (2 mA cm ⁻²)	[102]
	Graphene-like carbon	Large active surface area	–	≈100 h (1 mA cm ⁻²)	[101]
	Reduce graphene oxide	Large active surface area	–	≈300 h (1 mA cm ⁻²)	[98]
	Nitrogen-doped graphene oxide	anti-corrosion	–	≈1200 h (1 mA cm ⁻²)	[104]
	Highly viscoelastic polyvinyl butyral film (PVB)	Blocking H ₂ O, hydrophilicity	6.67 × 10 ⁻² mS cm ⁻¹ (1 μm)	≈2200 h (0.5 mA cm ⁻²)	[106]
	Nafion-Zn-X	Blocking SO ₄ ²⁻	6.13 mS cm ⁻¹ (10 μm)	10 000 cycles (5 mA cm ⁻²)	[110]
	Polyamide (PA)	Blocking H ₂ O/O ₂ , hydrophilicity	–	≈8000 h (0.5 mA cm ⁻²)	[105]
	Zinc perfluorinated sulfonic acid membrane (ZPSAM)	Anion matrix	1.17 mS cm ⁻¹ (23 μm)	2000 cycles (2 mA cm ⁻²)	[109]
	Polyacrylamide (PAM)/polyvinylpyrrolidone (PVP)	Hydrophilicity	–	≈2220 h (0.2 mA cm ⁻²)	[108]
	Silanization of (3-aminopropyl) triethoxysilane	Hydrophilicity	0.28 mS cm ⁻¹ (500 nm)	3500 h (2 mA cm ⁻²)	[134]
In situ formation layer	ZnF ₂	High ionic conductivity	≈10 ⁻⁴ mS cm ⁻¹ (16 μm)	≈700 h (0.5 mA cm ⁻²)	[119]
	ZnF ₂	High ionic conductivity	80.2 mS cm ⁻¹ (16 μm)	2500 h (1 mA cm ⁻²)	[118]
	ZnF ₂	High ionic conductivity	–	800 h (1 mA cm ⁻²)	[117]
	Indium hydroxide sulfate	High ionic conductivity	≈57 mS cm ⁻¹ (2.3 μm)	≈700 h (0.5 mA cm ⁻²)	[124]
	Zn ₄ SO ₄ (OH) ₆ ·5H ₂ O/Cu ₂ O	Uniform electric field distribution	–	1400 h (2 mA cm ⁻²)	[128]
	ZnP	High ionic conductivity	–	3300 h (5 mA cm ⁻²)	[120]
	Polydopamine	Blocking H ₂ O/O ₂ , hydrophilicity	1.1 × 10 ⁻² mS cm ⁻¹ (40 nm)	>1000 h (1 mA cm ⁻²)	[126]
	ZnSe	Cultivator, High ionic conductivity	–	1700 h (1 mA cm ⁻²)	[123]
	ZnSe	High ionic conductivity	1.7 × 10 ⁻² mS cm ⁻¹ (1.5 μm)	1530 h (1 mA cm ⁻²)	[122]
	ZnSe	High ionic conductivity	–	1500 h (10 mA cm ⁻²)	[121]
	Zn ₃ (PO ₄) ₂ -ZnF ₂ -ZnS	Multifunctional	9 × 10 ⁻² mS cm ⁻¹ (≈400 nm)	2500 h (1 mA cm ⁻²)	[127]
	ZnF ₂ /Zn ₃ (PO ₄) ₂ /CF _x	Multifunctional	2.23 × 10 ⁻² mS cm ⁻¹ (≈700 nm)	500 h (1 mA cm ⁻²)	[129]
	ZIF-8	Ordered nanochannels and N species	–	1200 h (2 mA cm ⁻²)	[114]
	MOF-derived carbon	Hydrophilicity, Large active surface area	–	>400 h (10 mA cm ⁻²)	[115]

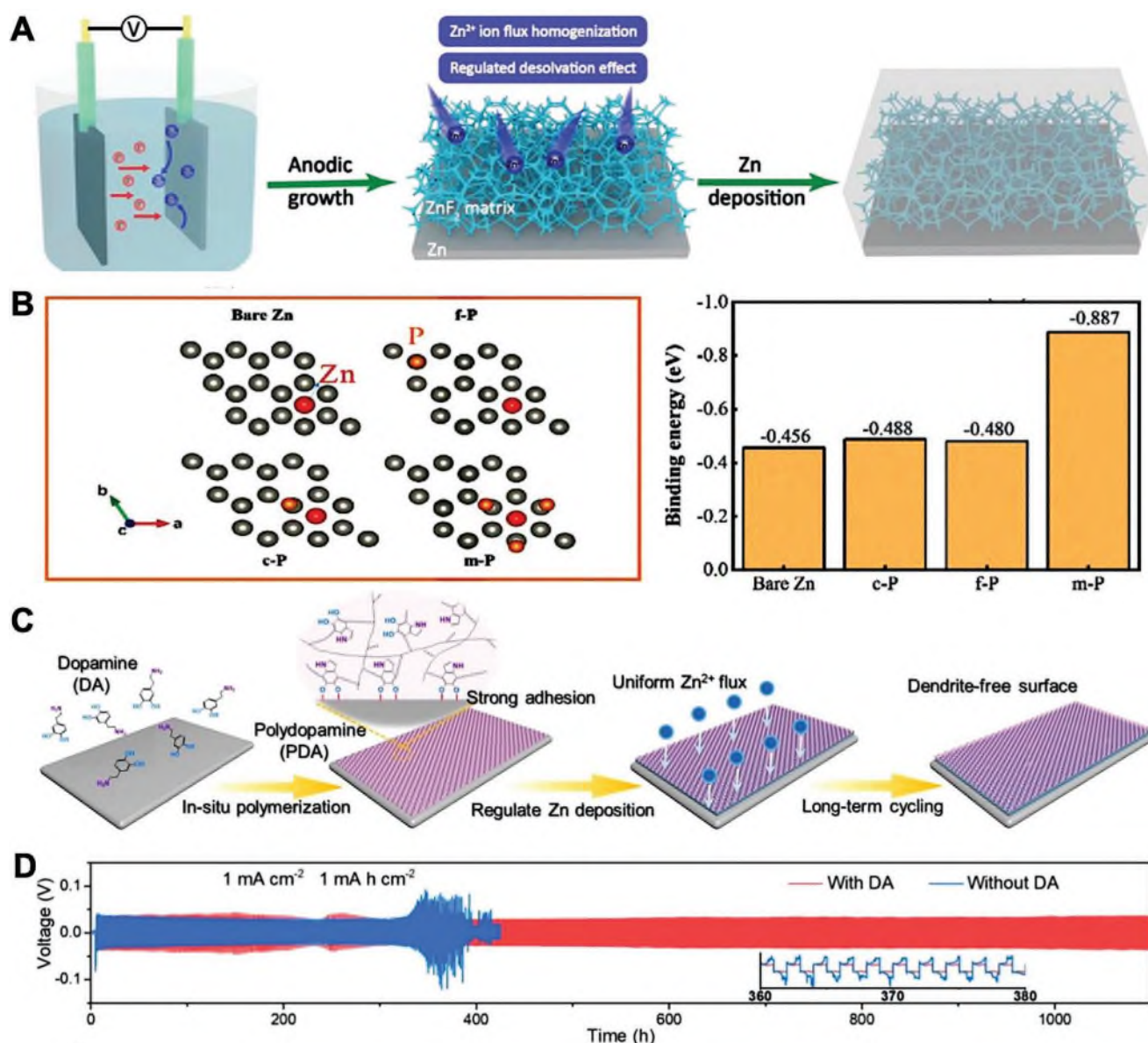


Figure 12. A) Schematic illustration of the fabrication of ZnF₂ coating. Reproduced with permission.^[177] Copyright 2021, Wiley-VCH. B) Zn adsorbed on bare Zn and ZnF₂ coating at different adsorption sites and the corresponding binding energy calculated by the DFT. Reproduced with permission.^[120] Copyright 2021, Wiley-VCH. C) Schematic illustration of the in situ formation of the polydopamine ultra-thin protective layer and its effective mechanism for dendrite-free Zn anode. D) Performance of Zn symmetric cells. Reproduced with permission.^[126] Copyright 2021, The Royal Society of Chemistry.

Besides, ZIF-8 derived carbon layer was prepared by Ruoff et al.^[115] The ZIF-8 derived carbon layer contains lots of N sites that can enhance the transport kinetics of Zn²⁺ ions. Importantly, the porous carbon layer retains a significant amount of -OH or -COOH, which along with N could provide active sites for Zn²⁺ ion to reside. As a result, the symmetric cell can cycle for over 400 h at 1–10 mA cm⁻² and the lifespan of full battery was longer than 5000 cycles at 1 C. In addition, the in situ ZnF₂ thin films also can be prepared by the thermal calcination strategy (Figure 13C).^[119] Passerini et al. found that the ZnF₂ can allow insertion of Zn²⁺ and offer diffusion channels for the transport to/from the Zn anode via an interstitial diffusion mechanism. Until now, a few hybrid

in situ formed protective coatings such as Zn₃(PO₄)₂-ZnF₂-ZnS have also been explored.^[127] They often exhibit higher ionic conductivity and corrosion potential than their individual components (e.g., ZnF₂, ZnS, or Zn₃(PO₄)₂), which show outstanding anti-corrosion ability and homogeneous Zn deposition for long cycling. However, the synergistic effect between different components of such hybrid layers should be further investigated. Compared to the layers formed by in situ electrochemical polymerization/deposition/conversion, the thermal treatment generated coatings do not possess the self-repairing function. The protective coatings may be broken and peeled off from the Zn anode after cycling for 1000 h, which leads to the performance decay.

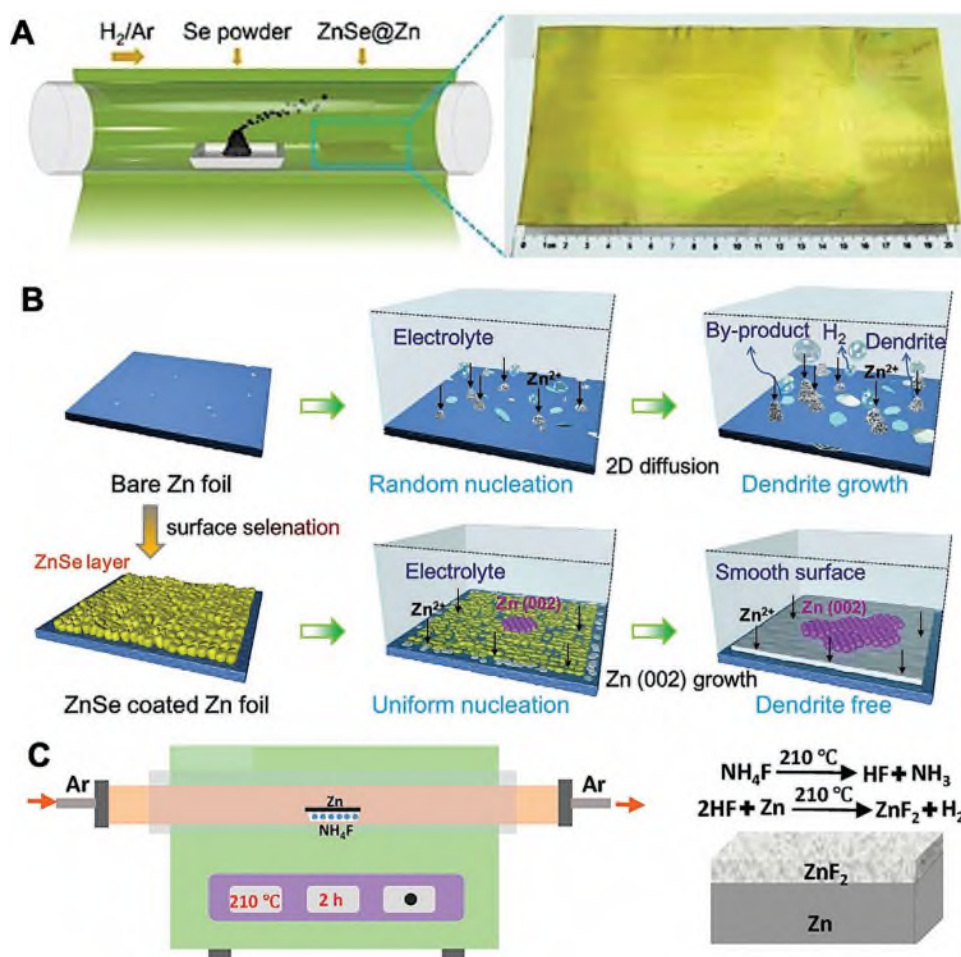


Figure 13. A) CVD growth of in situ formed ZnSe layer on Zn surface and corresponding photographs. B) Schematic diagram showing Zn deposition on bare Zn anode and ZnSe@Zn anode. Reproduced with permission.^[122] Copyright 2021, Wiley-VCH. C) Schematic illustration of the production of the artificial ZnF₂ layer. Reproduced with permission.^[119] Copyright 2021 American Chemical Society.

4.2.3. Chemically Generated Layers

Chemical reactions of Zn and other compounds can be utilized to synthesize functional protective layers. Pan et al. fabricated a zinc phosphate protective layer on the Zn foil by using a simple acid-etching approach (Figure 14A),^[116] which can enhance the Zn²⁺ ion kinetics and regulate the deposition/dissolution behaviors. At the same time, the acid etching of Zn generated a more compact layer, which mainly exposes Zn (002) plane that could induce lateral deposition of Zn. As a result, the Zn symmetric cells can be cycled for over than 3000 h at 1 mA cm⁻² and 0.5 mAh cm⁻² (Figure 14B). In addition, Cao et al. directly immersed the Zn foil into the weakly acidic aqueous solution of CuSO₄ for only 10–60 s to form a uniform and robust protective layer (Zn₄SO₄(OH)₆·5H₂O/Cu₂O), which enables uniform electric field distribution and controllable dendrite growth, leading to a long-term cycle life of over 1400 h.^[128] Compared to the ex situ formed layers, the in situ formed layers are still very limited and other functional in situ formed protective layers are urgently needed.

4.2.4. Other Strategies

The abovementioned synthetic methods can be combined to in situ generate protective layers with more complex composition and structure. For instance, a 3D stacked lamellar matrix composed of ZnF₂/Zn₃(PO₄)₂/CF_x was deposited onto Zn anode surface via thermal calcination and electrodeposition, delivering enhanced thermodynamic stability and rapid Zn²⁺ ion transport kinetics.^[129] The channels and functional sites can not only effectively uniform the Zn²⁺ ion flux to inhibit the Zn dendrite growth, but also eliminate the side reactions on the Zn anode surface to enhance the utilization of metallic Zn (Figure 14C). The reported in situ formed coating materials and their corresponding electrochemical performance are summarized in Table 3.

5. Electrolyte Engineering

In addition to designing the anode supports and protective layers, electrolyte engineering is another strategy to modify

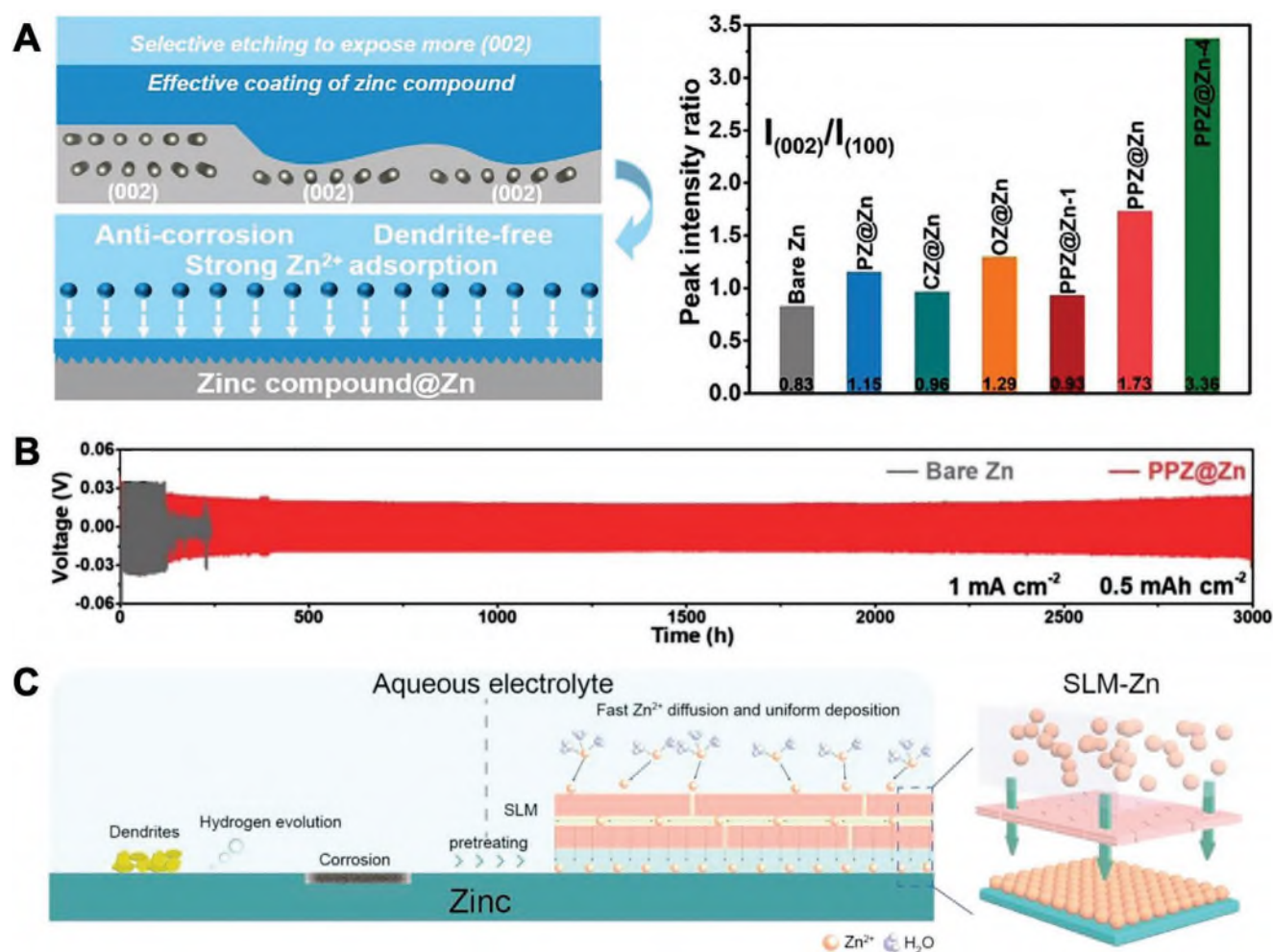


Figure 14. A) Schematic illustration of selective corrosion of crystal planes to fabricate the textured Zn electrodes with zinc compound coatings and corresponding XRD patterns. B) Performance of symmetric cells. Reproduced with permission.^[116] Copyright 2021, Wiley-VCH. C) The formation of hybrid $\text{ZnF}_2/\text{Zn}_3(\text{PO}_4)_2/\text{CFx}$ layer on Zn electrode and the surface chemistry on Zn electrodes. Reproduced with permission.^[129] Copyright 2021, Wiley-VCH.

the Zn surface or Zn/electrolyte interface. A direct way to tune the electrolyte property is to change the Zn salts. Organic salts such as $\text{Zn}(\text{TFSI})_2$ and $\text{Zn}(\text{CH}_3\text{COO})_2$ and inorganic salts such as ZnSO_4 , ZnCl_2 , $\text{Zn}(\text{NO}_3)_2$, and $\text{Zn}(\text{ClO}_4)_2$ are commonly used in ZIB electrolytes. The former helps to expand the voltage window of ZIBs and thus can achieve a high energy density,^[135] but the poor ionic conductivity and high cost limit their wide applications; whereas the latter is much cheaper yet the side reactions are more severe.^[136,137] Introducing additives is an effective way to eliminate the side reactions and dendrite growth, thus enhancing the lifespan of ZIBs.

Metal ions, polymer surfactants, and organic molecules have been added into liquid electrolytes to enhance the stability. For example, Niu et al. added NaSO_4 into the ZnSO_4 electrolyte to obtain a stable Zn surface as the lower reduction potential of Na^+ ion than Zn^{2+} ion avoids the Zn^{2+} ions deposition at high potentials (Figure 15A).^[138] The electrolyte can also prohibit cathode dissolution therefore enhances the stability of the full battery. In addition to inorganic salt additives, organic molecules such as diethyl ether (Et_2O) can be useful even with a low amount (e.g., 2 vol%). As shown in Figure 15B, the Et_2O can

effectively suppress the dendrite growth.^[139] The highly polarized Et_2O molecules would adsorb lots of electrons. Whereas the Zn^{2+} ions plating occurs at low-energy area where Et_2O layer does not exist. Therefore, Zn can be uniformly deposited at the anode surface that avoids the dendrite growth. To suppress the gas evolution, LiTFSI or other TFSI^- containing additives were added into Zn salt electrolytes, forming a solvation sheath structure of $(\text{Zn-TFSI})^+$ instead of $(\text{Zn}(\text{H}_2\text{O})_6)^{2+}$ that alleviates corrosion and passivation. What is more, Cui et al. prepared the “Water-in-deep eutectic solvent” (DES) electrolytes by hybridizing the LiTFSI and $\text{Zn}(\text{TFSI})_2$ with urea. The DES electrolyte can induce water molecules to participate in DES’s internal interaction (H bonds and coordination bonds) network, which would eliminate the reaction between water molecules and Zn metal (Figure 15C). Furthermore, Zn dendrite growth and gas evolution can be inhibited, leading to improved Coulombic efficiency and capacity of ZIBs.^[140] Acetamide- $\text{Zn}(\text{TFSI})_2$ eutectic electrolyte can also prohibit side reactions and dendrite growth.^[141] The electrolyte additive can effectively enhance the performance of ZIBs by improving the stability of the Zn/electrolyte interface. However, the actual operating

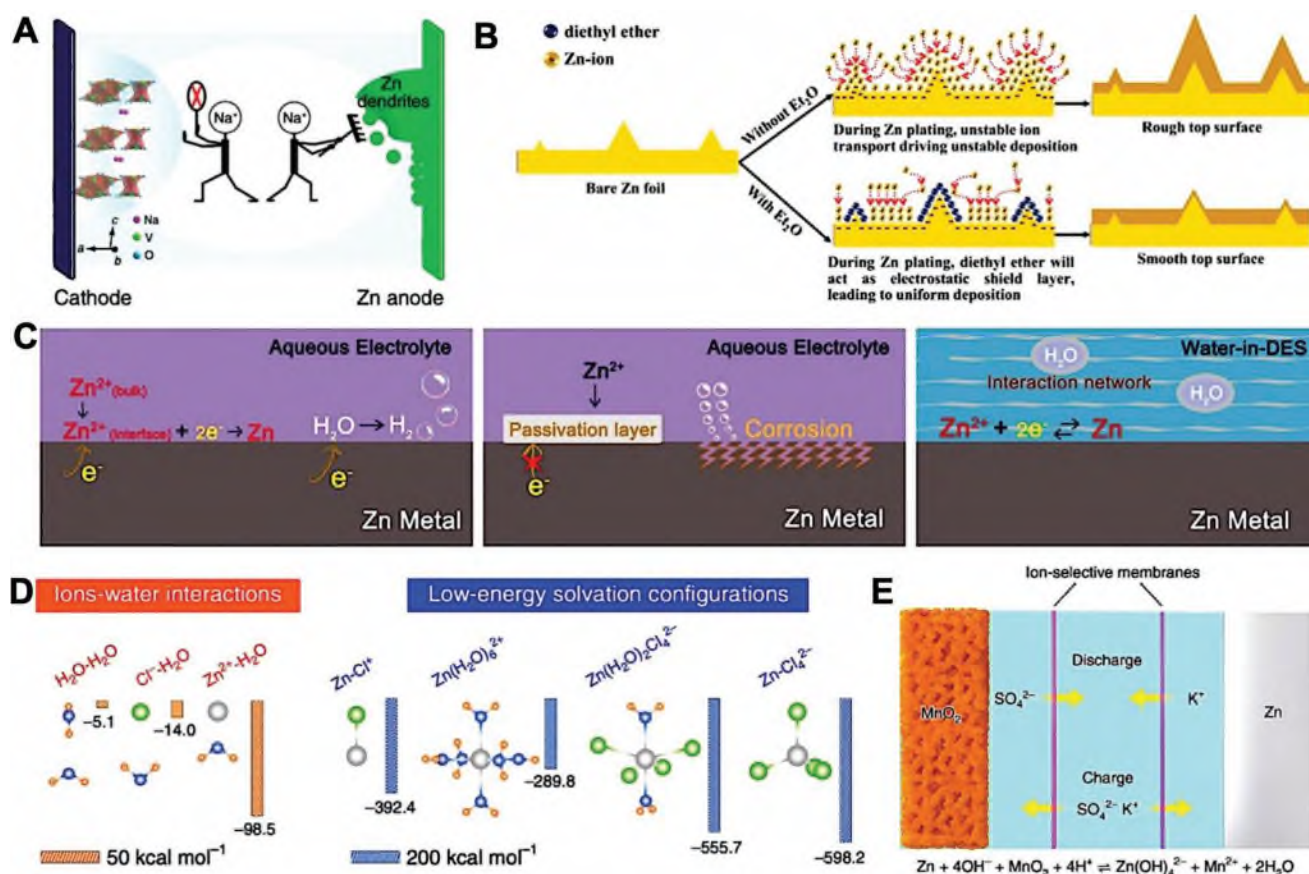


Figure 15. A) Na₂SO₄ additive suppresses the dissolution of NaV₃O₈·1.5H₂O (NVO) nanobelts and the formation of Zn dendrites. Reproduced with permission.^[138] Copyright 2018, Springer Nature. B) Morphology evolution of Zn anodes in mild aqueous electrolyte with and without Et₂O additive during Zn stripping/plating. Reproduced with permission.^[139] Copyright 2018, Elsevier. C) Reactions on Zn anode surface in the traditional and water-in-DES aqueous electrolytes. Reproduced with permission.^[140] Copyright 2019, Elsevier. D) The interaction between Zn²⁺ ions and H₂O, and the formation energies of Zn²⁺ ion solvation configurations. Reproduced with permission.^[145] Copyright 2020, Springer Nature. E) The ZIB structure and decoupled reactions at the cathode and anode. Reproduced with permission.^[147] Copyright 2020, Springer Nature.

voltage and capacity of ZIBs are still far lower than the theoretical values due to the energy transformation efficiency of anode and cathode. In addition to the LiTFSI, LiPF₆ was also explored as an electrolyte additive; it can effectively prohibit the decomposition of Zn(TFSI)₂ and enhance the voltage window of ZIBs.^[142] Strong adsorption and 2D diffusion of Zn²⁺ ions on Zn anode in aqueous electrolyte without limits are critical gradients for dendrite growth. Polyethylene-glycol (PEG) is an excellent polymer additive for guiding the Zn²⁺ ion diffusion in a long 3D pathway to avoid dendrite growth.^[143] In addition, a hybrid electrolyte such as Zn(TFSI)₂-triethyl phosphate electrolyte can improve the lifespan of Zn symmetric cell.^[144]

Electrolyte concentration also changes the solvation structure of Zn²⁺ ions and other anions, which further affects the Zn²⁺ ions deposition behavior. It can be explained by the different ionic conductivity and binding energy of Zn²⁺/Zn anode surface. Chen et al. used high concentration ZnCl₂ electrolytes for ZIBs. Long lifespan was achieved at ultralow temperature. In the electrolyte, water would not freeze due to the lack of H bonds, which were broken by the Zn²⁺ ions due to the stronger binding energy of Zn²⁺-H₂O (−98.5 kcal mol^{−1} versus −5.1 kcal mol^{−1} for H₂O-H₂O) (Figure 15D).^[145] Nonetheless, free water still

exists in concentrated electrolytes (e.g., 1 M LiTFSI, 20 M Zn(TFSI)₂).^[146] Hu et al. used decoupled electrolytes to increase the operating voltage window and capacity of the Zn-MnO₂ battery (Figure 15E).^[147] The architecture of the battery is composed of anode (alkaline electrolyte), cathode (acid electrolyte), and electrolyte (K₂SO₄ solution). The unique design guarantees the complete usage of the active electrode materials. The open-circuit voltage was increased from 1.5 to 2.83 V, which further enhances the energy density of ZIBs. The full battery capacity was ≈600 mAh g^{−1}, close to the theoretical values. The battery also possessed good stability with a capacity degradation less than 2% after 200 h cycling. Although the electrolyte formulation can effectively inhibit the dendrite growth and side reactions, the depletion of electrolyte is a critical issue for the commercialization.

6. Conclusion and Perspective

In conclusion, this review has summarized the recent progress in the surface and interface engineering of Zn anodes with an emphasis on the support and protective layer design. In

general, the support materials for Zn^{2+} ion stripping/plating processes should possess a continuous and stable skeleton, low nucleation barrier, high electronic conductivity, no galvanic corrosion, and high porosity/surface area. The uniform electric field distribution and low current density on the Zn surface can avoid charge accumulation on Zn anodes. Whereas the surface protective layers should be able to tune the interfacial properties and thus suppress the side reaction and guide the homogeneous Zn deposition. Although significant progress has been achieved, there are still many obstacles. With the requirements of high-performance Zn anode and their application in mind, perspectives are listed as follows.

- 1) Functional supports for Zn anodes: With commercialization in mind, support materials should be urgently developed for stable, lightweight, and dendrite-free Zn anodes. At the same time, it is also essential to develop flexible support materials for wearable electronics; the ideal support materials should be non-toxic, eco-friendly, low-cost, and mechanically robust.
- 2) Stable and ultra-thin protective coatings for Zn anodes: Protective layers with deliberately designed structures and high ionic conductivity can prevent Zn^{2+} ions from depositing on charge accumulated area and guide Zn^{2+} ions to transfer through well-defined ionic channels. To prepare precise structures and support large-scale applications, advanced methods to fabricate functional and binder-free protective layers should be explored in the future, such as 3D printing, laser etching, magnetron sputtering, etc. New materials such as MXenes, ceramic coatings (carbides), hybrid materials should also be explored as protective layers for Zn anodes.
- 3) Theoretical modeling: Standard theoretical models for the Zn^{2+} stripping/plating processes on anode are constantly referenced in ZIBs with alkaline electrolytes systems or Li-ion batteries. Therefore, the Zn^{2+} ion deposition mechanisms in mild acidic should be investigated by combining the advanced in situ observation technologies and theoretical calculations. The universal theory model of ion diffusion, dendrites growth and corresponding conditions, and hydrogen evolution process should be built.
- 4) Applications of ZIBs: Designing micro ZIBs for wearable electronics and high-performance ZIBs for traffic tools may be suitable targets. At the same time, soft package cells are considered next-generation power for electric vehicles or large-scale energy storage stations. However, few amplifying ZIBs (refer to existing battery size for electric cars) with long lifespan (>1000 h) have been successfully realized for practical applications. Therefore, long lifespan Zn anode for large ZIBs is urgently to be investigated in the future.

Acknowledgements

The authors thank the National Natural Science Foundation of China (No. 22001081, 22075236) and Xiamen University for support.

Conflict of Interest

The authors declare no conflict of interest.

Keywords

interface engineering, protective coating, support materials, surface engineering, zinc-ion batteries

Received: January 1, 2022

Revised: February 10, 2022

Published online:

- [1] X. Ji, *Energy Environ. Sci.* **2019**, 12, 3203.
- [2] E. Pomerantseva, F. Bonaccorso, X. Feng, Y. Cui, Y. Gogotsi, *Science* **2019**, 366, 8285.
- [3] Y. Shao, M. F. El-Kady, J. Sun, Y. Li, Q. Zhang, M. Zhu, H. Wang, B. Dunn, R. B. Kaner, *Chem. Rev.* **2018**, 118, 9233.
- [4] G. Fang, J. Zhou, A. Pan, S. Liang, *ACS Energy Lett.* **2018**, 3, 2480.
- [5] A. Konarov, N. Voronina, J. H. Jo, Z. Bakenov, Y.-K. Sun, S.-T. Myung, *ACS Energy Lett.* **2018**, 3, 2620.
- [6] J. F. Parker, J. S. Ko, D. R. Rolison, J. W. Long, *Joule* **2018**, 2, 2519.
- [7] S. Wang, W. Ma, Z. Sang, F. Hou, W. Si, J. Guo, J. Liang, *J. Energy Chem.* **2022**, 67, 82.
- [8] D. Liu, Y. Tong, X. Yan, J. Liang, S. X. Dou, *Batteries Supercaps* **2019**, 2, 743.
- [9] J. Ming, J. Guo, C. Xia, W. Wang, H. N. Alshareef, *Mater. Sci. Eng., R* **2019**, 135, 58.
- [10] P. He, Q. Chen, M. Yan, X. Xu, L. Zhou, L. Mai, C.-W. Nan, *Energy-Chem* **2019**, 1, 100022.
- [11] H. F. Li, L. T. Ma, C. P. Han, Z. F. Wang, Z. X. Liu, Z. J. Tang, C. Y. Zhi, *Nano Energy* **2019**, 62, 550.
- [12] D. Selvakumaran, A. Pan, S. Liang, G. Cao, *J. Mater. Chem. A* **2019**, 7, 18209.
- [13] X. Zeng, J. Hao, Z. Wang, J. Mao, Z. Guo, *Energy Storage Mater.* **2019**, 20, 410.
- [14] J. Cao, D. Zhang, X. Zhang, Z. Zeng, J. Qin, Y. Huang, *Energy Environ. Sci.* **2022**, 15, 499.
- [15] B. Li, X. Zhang, T. Wang, Z. He, B. Lu, S. Liang, J. Zhou, *Nano-Micro Lett.* **2021**, 14, 6.
- [16] L. Geng, X. Wang, K. Han, P. Hu, L. Zhou, Y. Zhao, W. Luo, L. Mai, *ACS Energy Lett.* **2021**, 7, 247.
- [17] C. Liu, X. Xie, B. Lu, J. Zhou, S. Liang, *ACS Energy Lett.* **2021**, 6, 1015.
- [18] J. Shin, J. Lee, Y. Park, J. W. Choi, *Chem. Sci.* **2020**, 11, 2028.
- [19] Q. Zhang, J. Luan, Y. Tang, X. Ji, H. Wang, *Angew. Chem., Int. Ed.* **2020**, 59, 131801.
- [20] C. Han, W. Li, H. K. Liu, S. Dou, J. Wang, *Nano Energy* **2020**, 74, 104880.
- [21] Y. Yu, W. Xu, X. Liu, X. Lu, *Adv. Sustainable Syst.* **2020**, 4, 2000082.
- [22] Z. Yi, G. Chen, F. Hou, L. Wang, J. Liang, *Adv. Energy Mater.* **2021**, 11, 2003065.
- [23] Q. Zhang, J. Luan, Y. Tang, X. Ji, H. Wang, *Angew. Chem., Int. Ed.* **2020**, 59, 13180.
- [24] W. Lu, C. Zhang, H. Zhang, X. Li, *ACS Energy Lett.* **2021**, 6, 2765.
- [25] Q. Yang, G. J. Bang, Y. Guo, Z. X. Liu, B. X. Yon, D. H. Wang, Z. D. Huang, X. L. Li, J. Fan, C. Y. Zhi, *Adv. Mater.* **2019**, 31, 1903778.
- [26] M. Li, J. Lu, X. Ji, Y. Li, Y. Shao, Z. Chen, C. Zhong, K. Amine, *Nat. Rev. Mater.* **2020**, 5, 276.
- [27] C. A. Laska, M. Auinger, P. U. Biedermann, D. Iqbal, N. Laska, J. De Strycker, K. J. J. Mayrhofer, *Electrochim. Acta* **2015**, 159, 198.
- [28] H. He, H. Qin, J. Wu, X. Chen, R. Huang, F. Shen, Z. Wu, G. Chen, S. Yin, J. Liu, *Energy Storage Mater.* **2021**, 43, 317.
- [29] C. Li, X. Xie, S. Liang, J. Zhou, *Energy Environ. Sci.* **2020**, 3, 146.
- [30] W. Wang, G. Huang, Y. Wang, Z. Cao, L. Cavallo, M. N. Hedhili, H. N. Alshareef, *Adv. Energy Mater.* **2022**, 12, 2102797.

- [31] G. Li, Z. Liu, Q. Huang, Y. Gao, M. Regula, D. Wang, L.-Q. Chen, D. Wang, *Nat. Energy* **2018**, 3, 1076.
- [32] Z. Cao, P. Zhuang, X. Zhang, M. Ye, J. Shen, P. M. Ajayan, *Adv. Energy Mater.* **2020**, 10, 2001599.
- [33] K. Yan, Z. Lu, H. Lee, F. Xiong, P. C. Hsu, Y. Li, J. Zhao, S. Chu, Y. Cui, *Nat. Energy* **2016**, 1, 1.
- [34] Y. Xu, Y. Zhang, Z. Guo, J. Ren, Y. Wang, H. Peng, *Angew. Chem., Int. Ed.* **2015**, 54, 15390.
- [35] Y. Liu, X. Chi, Q. Han, Y. Du, J. Huang, Y. Liu, J. Yang, *J. Power Sources* **2019**, 443, 227244.
- [36] M. Nakayama, S. Osae, K. Kaneshige, K. Komine, H. Abe, *J. Electrochem. Soc.* **2016**, 163, A2340.
- [37] M. Bai, K. Xie, K. Yuan, K. Zhang, N. Li, C. Shen, Y. Lai, R. Vajtai, P. Ajayan, B. Wei, *Adv. Mater.* **2018**, 29, 1801213.
- [38] Z. Huang, X. Qin, G. Li, W. Yao, J. Liu, N. Wang, K. Ithisuphalap, G. Wu, M. Shao, Z. Shi, *ACS Appl. Energy Mater.* **2019**, 2, 4428.
- [39] A. Pendashteh, J. Palma, M. Anderson, J. J. Vilatela, R. Marcilla, *ACS Appl. Energy Mater.* **2018**, 1, 2434.
- [40] M. Ren, J. Zhang, J. M. Tour, *ACS Appl. Energy Mater.* **2019**, 2, 1460.
- [41] Y. Zeng, X. Zhang, R. Qin, X. Liu, P. Fang, D. Zheng, Y. Tong, X. Lu, *Adv. Mater.* **2019**, 31, 1903675.
- [42] S. Zhai, N. Wang, X. Tan, K. Jiang, Z. Quan, Y. Li, Z. Li, *Adv. Funct. Mater.* **2021**, 31, 2008894.
- [43] J. H. Lee, R. Kim, S. Kim, J. Heo, H. Kwon, J. H. Yang, H. T. Kim, *Energy Environ. Sci.* **2020**, 13, 2839.
- [44] F. Xie, H. Li, X. Wang, X. Zhi, D. Chao, K. Davey, S. Z. Qiao, *Adv. Energy Mater.* **2021**, 11, 2003419.
- [45] C. Uthaisar, V. Barone, J. E. Peralta, *J. Appl. Phys.* **2009**, 106, 113715.
- [46] R. Zhang, X. R. Chen, X. Chen, X. B. Cheng, X. Q. Zhang, C. Yan, Q. Zhang, *Angew. Chem., Int. Ed.* **2017**, 56, 7764.
- [47] X. Wu, J. J. Hong, W. Shin, L. Ma, T. Liu, X. Bi, Y. Yuan, Y. Qi, T. W. Surta, W. Huang, *Nat. Energy* **2019**, 4, 123.
- [48] J. Zheng, Q. Zhao, T. Tang, J. Yin, C. D. Quilty, G. D. Renderos, X. Liu, Y. Deng, L. Wang, D. C. J. S. Bock, *Science* **2019**, 366, 645.
- [49] J. Zheng, D. C. Bock, T. Tang, Q. Zhao, J. Yin, K. R. Tallman, G. Wheeler, X. Liu, Y. Deng, S. Jin, A. C. Marschilok, E. S. Takeuchi, K. J. Takeuchi, L. A. Archer, *Nat. Energy* **2021**, 6, 398.
- [50] G. Zhang, X. Zhang, H. Liu, J. Li, Y. Chen, H. Duan, *Adv. Energy Mater.* **2021**, 11, 2003927.
- [51] Z. Kang, C. Wu, L. Dong, W. Liu, J. Mou, J. Zhang, Z. Chang, B. Jiang, G. Wang, F. Kang, C. Xu, *ACS Sustainable Chem. Eng.* **2019**, 7, 3364.
- [52] X. Shi, G. Xu, S. Liang, C. Li, S. Guo, X. Xie, X. Ma, J. Zhou, *ACS Sustainable Chem. Eng.* **2019**, 7, 17737.
- [53] Q. Zhang, J. Luan, L. Fu, S. Wu, Y. Tang, X. Ji, H. Wang, *Angew. Chem., Int. Ed.* **2019**, 58, 15841.
- [54] Q. Li, Y. Wang, F. Mo, D. Wang, G. Liang, Y. Zhao, Q. Yang, Z. Huang, C. Zhi, *Adv. Energy Mater.* **2021**, 11, 2003931.
- [55] Y. An, Y. Tian, S. Xiong, J. Feng, Y. Qian, *ACS Nano* **2021**, 15, 11828.
- [56] S. Wang, Z. Wang, Y. Yin, T. Li, N. Chang, F. Fan, H. Zhang, X. Li, *Energy Environ. Sci.* **2021**, 14, 4077.
- [57] D. Mackinnon, J. Brannen, P. L. Fenn, *J. Appl. Electrochem.* **1987**, 17, 1129.
- [58] Q. Li, Y. Zhao, F. Mo, D. Wang, Q. Yang, Z. Huang, G. Liang, A. Chen, C. Zhi, *EcoMat* **2020**, 2, 12035.
- [59] J. Cao, D. Zhang, C. Gu, X. Wang, S. Wang, X. Zhang, J. Qin, Z. S. Wu, *Adv. Energy Mater.* **2021**, 11, 2101299.
- [60] P. Zou, Y. Sui, H. Zhan, C. Wang, H. L. Xin, H. M. Cheng, F. Kang, C. Yang, *Chem. Rev.* **2021**, 121, 5986.
- [61] M. Zhou, S. Guo, J. Li, X. Luo, Z. Liu, T. Zhang, X. Cao, M. Long, B. Lu, A. Pan, G. Fang, J. Zhou, S. Liang, *Adv. Mater.* **2021**, 33, 2100187.
- [62] R. Ramanauskas, *Appl. Surf. Sci.* **1999**, 153, 53.
- [63] P. Seré, J. D. Culcasi, C. I. Elsner, A. R. Di Sarli, *Surf. Coat. Technol.* **1999**, 122, 143.
- [64] J. Zheng, Y. Deng, J. Yin, T. Tang, R. Garcia-Mendez, Q. Zhao, L. A. Archer, *Adv. Mater.* **2021**, 34, 2106867.
- [65] Y. Zhang, J. D. Howe, S. Ben-Yoseph, Y. Wu, N. Liu, *ACS Energy Lett.* **2021**, 6, 404.
- [66] L. Wang, W. Huang, W. Guo, Z. H. Guo, C. Chang, L. Gao, X. Pu, *Adv. Funct. Mater.* **2021**, 32, 2108533.
- [67] T. Chen, Y. Wang, Y. Yang, F. Huang, M. Zhu, B. T. W. Ang, J. M. Xue, *Adv. Funct. Mater.* **2021**, 31, 2101607.
- [68] Z. Qi, T. Xiong, T. Chen, C. Yu, M. Zhang, Y. Yang, Z. Deng, H. Xiao, W. S. V. Lee, J. Xue, *ACS Appl. Mater. Interfaces* **2021**, 13, 28129.
- [69] Z. Chen, C. Li, Q. Yang, D. Wang, X. Li, Z. Huang, G. Liang, A. Chen, C. Zhi, *Adv. Mater.* **2021**, 33, 2105426.
- [70] S. Wang, Q. Ran, R. Yao, H. Shi, Z. Wen, M. Zhao, X. Lang, Q. Jiang, *Nat. Commun.* **2020**, 11, 1634.
- [71] B. Liu, S. Wang, Z. Wang, H. Lei, Z. Chen, W. Mai, *Small* **2020**, 16, 2001323.
- [72] J. Zhou, M. Xie, F. Wu, Y. Mei, Y. Hao, L. Li, R. Chen, *Adv. Mater.* **2021**, 34, 2106897.
- [73] J. Zheng, Q. Zhao, T. Tang, J. Yin, C. D. Quilty, G. D. Renderos, X. Liu, Y. Deng, L. Wang, D. Bock, *Science* **2019**, 366, 645.
- [74] M. Li, J. Meng, Q. Li, M. Huang, X. Liu, K. A. Owusu, Z. Liu, L. Mai, *Adv. Funct. Mater.* **2018**, 28, 1802016.
- [75] A.-R. El-Sayed, H. S. Mohran, H. M. A. El-Lateef, *Metall. Mater. Trans. A* **2011**, 43, 619.
- [76] Y. Tian, Y. An, C. Wei, B. Xi, S. Xiong, J. Feng, Y. Qian, *ACS Nano* **2019**, 13, 11676.
- [77] Z. Wang, J. Huang, Z. Guo, X. Dong, Y. Liu, Y. Wang, Y. Xia, *Joule* **2019**, 3, 1289.
- [78] Y. Zuo, K. Wang, P. Pei, M. Wei, X. Liu, Y. Xiao, P. Zhang, *Mater. Today Energy* **2021**, 20, 100692.
- [79] J. Wang, Y. Yang, Y. Zhang, Y. Li, R. Sun, Z. Wang, H. Wang, *Energy Storage Mater.* **2021**, 35, 19.
- [80] H. Yan, S. Li, Y. Nan, S. Yang, B. Li, *Adv. Energy Mater.* **2021**, 11, 2100186.
- [81] K. Wu, J. Yi, X. Liu, Y. Sun, J. Cui, Y. Xie, Y. Liu, Y. Xia, J. Zhang, *Nano-Micro Lett.* **2021**, 13, 79.
- [82] X. Xie, S. Liang, J. Gao, S. Guo, J. Guo, C. Wang, G. Xu, X. Wu, G. Chen, J. Zhou, *Energy Environ. Sci.* **2020**, 13, 503.
- [83] Q. Zhang, J. Luan, X. Huang, Q. Wang, D. Sun, Y. Tang, X. Ji, H. Wang, *Nat. Commun.* **2020**, 11, 3961.
- [84] L. Kang, M. Cui, F. Jiang, Y. Gao, H. Luo, J. Liu, W. Liang, C. Zhi, *Adv. Energy Mater.* **2018**, 8, 1801090.
- [85] P. Liang, J. Yi, X. Liu, K. Wu, Z. Wang, J. Cui, Y. Liu, Y. Wang, Y. Xia, J. Zhang, *Adv. Funct. Mater.* **2020**, 30, 1908528.
- [86] H. B. He, H. Tong, X. Y. Song, X. P. Song, J. Liu, *J. Mater. Chem. A* **2020**, 8, 7836.
- [87] C. Deng, X. Xie, J. Han, Y. Tang, J. Gao, C. Liu, X. Shi, J. Zhou, S. Liang, *Adv. Funct. Mater.* **2020**, 30, 2000599.
- [88] K. Zhao, C. Wang, Y. Yu, M. Yan, Q. Wei, P. He, Y. Dong, Z. Zhang, X. Wang, L. Mai, *Adv. Mater. Interfaces* **2018**, 5, 1800848.
- [89] R. Zhao, Y. Yang, G. Liu, R. Zhu, J. Huang, Z. Chen, Z. Gao, X. Chen, L. Qie, *Adv. Funct. Mater.* **2020**, 31, 2001867.
- [90] S. Yuan, L. Feng, K. Wang, J. Pang, M. Bosch, C. Lollar, Y. Sun, J. Qin, X. Yang, P. Zhang, Q. Wang, L. Zou, Y. Zhang, L. Zhang, Y. Fang, J. Li, H. C. Zhou, *Adv. Mater.* **2018**, 30, 1704303.
- [91] J. Meng, X. Liu, C. Niu, Q. Pang, J. Li, F. Liu, Z. Liu, L. Mai, *Chem. Soc. Rev.* **2020**, 49, 3142.
- [92] M. Liu, L. Yang, H. Liu, A. Amine, Q. Zhao, Y. Song, J. Yang, K. Wang, F. Pan, *ACS Appl. Mater. Interfaces* **2019**, 11, 32046.
- [93] H. Yang, Z. Chang, Y. Qiao, H. Deng, X. Mu, P. He, H. Zhou, *Angew. Chem., Int. Ed.* **2020**, 59, 9377.
- [94] X. Pu, B. Jiang, X. Wang, W. Liu, L. Dong, F. Kang, C. Xu, *Nano-Micro Lett.* **2020**, 12, 152.

- [95] M. Cui, Y. Xiao, L. Kang, W. Du, Y. Gao, X. Sun, Y. Zhou, X. Li, H. Li, F. Jiang, C. Zhi, *ACS Appl. Energy Mater.* **2019**, 2, 6490.
- [96] D. Han, S. Wu, S. Zhang, Y. Deng, C. Cui, L. Zhang, Y. Long, H. Li, Y. Tao, Z. Weng, Q. H. Yang, F. Kang, *Small* **2020**, 16, 2001736.
- [97] J. Zheng, Z. Huang, Y. Zeng, W. Liu, B. Wei, Z. Qi, Z. Wang, C. Xia, H. Liang, *Nano Lett.* **2022**, 22, 1017.
- [98] A. Xia, X. Pu, Y. Tao, H. Liu, Y. Wang, *Appl. Surf. Sci.* **2019**, 481, 852.
- [99] C. Shen, X. Li, N. Li, K. Xie, J. G. Wang, X. Liu, B. Wei, *ACS Appl. Mater. Interfaces* **2018**, 10, 25446.
- [100] W. Lee, J. Kim, S. Yun, W. Choi, H. Kim, W.-S. Yoon, *Energy Environ. Sci.* **2020**, 13, 4406.
- [101] Y. Wu, M. Wang, Y. Tao, K. Zhang, M. Cai, Y. Ding, X. Liu, T. Hayat, A. Alsaedi, S. Dai, *Adv. Funct. Mater.* **2019**, 30, 1907120.
- [102] Q. Yang, Y. Guo, B. Yan, C. Wang, Z. Liu, Z. Huang, Y. Wang, Y. Li, H. Li, L. Song, J. Fan, C. Zhi, *Adv. Mater.* **2020**, 32, 2001755.
- [103] W. Li, K. Wang, M. Zhou, H. Zhan, S. Cheng, K. Jiang, *ACS Appl. Mater. Interfaces* **2018**, 10, 22059.
- [104] J. Zhou, M. Xie, F. Wu, Y. Mei, Y. Hao, R. Huang, G. Wei, A. Liu, L. Li, R. Chen, *Adv. Mater.* **2021**, 33, 2101649.
- [105] Z. Zhao, J. Zhao, Z. Hu, J. Li, J. Li, Y. Zhang, C. Wang, G. Cui, *Energy Environ. Sci.* **2019**, 12, 1938.
- [106] J. Hao, X. Li, S. Zhang, F. Yang, X. Zeng, S. Zhang, G. Bo, C. Wang, Z. Guo, *Adv. Funct. Mater.* **2020**, 30, 2001263.
- [107] Z. Hong, Z. Ahmad, V. Viswanathan, *ACS Energy Lett.* **2020**, 5, 2466.
- [108] Z. Li, W. Deng, C. Li, W. Wang, Z. Zhou, Y. Li, X. Yuan, J. Hu, M. Zhang, J. Zhu, W. Tang, X. Wang, R. Li, *J. Mater. Chem. A* **2020**, 8, 17725.
- [109] Y. Cui, Q. Zhao, X. Wu, Z. Wang, R. Qin, Y. Wang, M. Liu, Y. Song, G. Qian, Z. Song, L. Yang, F. Pan, *Energy Storage Mater.* **2020**, 27, 1.
- [110] Y. Cui, Q. Zhao, X. Wu, X. Chen, J. Yang, Y. Wang, R. Qin, S. Ding, Y. Song, J. Wu, K. Yang, Z. Wang, Z. Mei, Z. Song, H. Wu, Z. Jiang, G. Qian, L. Yang, F. Pan, *Angew. Chem., Int. Ed.* **2020**, 59, 16594.
- [111] B. B. Wei, H. F. Liang, D. F. Zhang, Z. T. Wu, Z. B. Qi, Z. C. Wang, *J. Mater. Chem. A* **2017**, 5, 2844.
- [112] M.-S. Balogun, W. Qiu, W. Wang, P. Fang, X. Lu, Y. Tong, *J. Mater. Chem. A* **2015**, 3, 1364.
- [113] J. Zheng, Z. Cao, F. Ming, H. Liang, Z. Qi, W. Liu, C. Xia, C. Chen, L. Cavallo, Z. Wang, H. N. Alshareef, *ACS Energy Lett.* **2022**, 7, 197.
- [114] X. Liu, F. Yang, W. Xu, Y. Zeng, J. He, X. Lu, *Adv. Sci.* **2020**, 7, 2002173.
- [115] R. Yuksel, O. Buyukcikir, W. K. Seong, R. S. Ruoff, *Adv. Energy Mater.* **2020**, 10, 1904215.
- [116] X. Wang, J. Meng, X. Lin, Y. Yang, S. Zhou, Y. Wang, A. Pan, *Adv. Funct. Mater.* **2021**, 31, 2106114.
- [117] Y. Yang, C. Liu, Z. Lv, H. Yang, Y. Zhang, M. Ye, L. Chen, J. Zhao, C. C. Li, *Adv. Mater.* **2021**, 33, 2007388.
- [118] L. T. Ma, Q. Li, Y. R. Ying, F. X. Ma, S. M. Chen, Y. Y. Li, H. T. Huang, C. Y. Zhi, *Adv. Mater.* **2021**, 33, 2007406.
- [119] J. Han, H. Euchner, M. Kuenzel, S. M. Hosseini, A. Groß, A. Varzi, S. Passerini, *ACS Energy Lett.* **2021**, 6, 3063.
- [120] P. Cao, X. Zhou, A. Wei, Q. Meng, H. Ye, W. Liu, J. Tang, J. Yang, *Adv. Funct. Mater.* **2021**, 31, 2100398.
- [121] L. Zhang, B. Zhang, T. Zhang, T. Li, T. Shi, W. Li, T. Shen, X. Huang, J. Xu, X. Zhang, Z. Wang, Y. Hou, *Adv. Funct. Mater.* **2021**, 31, 2100186.
- [122] X. Yang, C. Li, Z. Sun, S. Yang, Z. Shi, R. Huang, B. Liu, S. Li, Y. Wu, M. Wang, Y. Su, S. Dou, J. Sun, *Adv. Mater.* **2021**, 33, 2105951.
- [123] T. C. Li, Y. V. Lim, X. Xie, X. L. Li, G. Li, D. Fang, Y. Li, Y. S. Ang, L. K. Ang, H. Y. Yang, *Small* **2021**, 17, 2101728.
- [124] Z. Cai, Y. Ou, B. Zhang, J. Wang, L. Fu, M. Wan, G. Li, W. Wang, L. Wang, J. Jiang, Z. W. Seh, E. Hu, X. Q. Yang, Y. Cui, Y. Sun, *J. Am. Chem. Soc.* **2021**, 143, 3143.
- [125] Y. Wang, Y. Chen, W. Liu, X. Ni, P. Qing, Q. Zhao, W. Wei, X. Ji, J. Ma, L. Chen, *J. Mater. Chem. A* **2021**, 9, 8452.
- [126] X. Zeng, K. Xie, S. Liu, S. Zhang, J. Hao, J. Liu, W. K. Pang, J. Liu, P. Rao, Q. Wang, J. Mao, Z. Guo, *Energy Environ. Sci.* **2021**, 14, 5947.
- [127] S. Di, X. Nie, G. Ma, W. Yuan, Y. Wang, Y. Liu, S. Shen, N. Zhang, *Energy Storage Mater.* **2021**, 43, 375.
- [128] X. Xu, Y. Chen, D. Zheng, P. Ruan, Y. Cai, X. Dai, X. Niu, C. Pei, W. Shi, W. Liu, F. Wu, Z. Pan, H. Li, X. Cao, *Small* **2021**, 17, 2101901.
- [129] S. Wu, S. Zhang, Y. Chu, Z. Hu, J. Luo, *Adv. Funct. Mater.* **2021**, 31, 2107397.
- [130] M. Zhou, S. Guo, G. Fang, H. Sun, X. Cao, J. Zhou, A. Pan, S. Liang, *J. Energy Chem.* **2021**, 55, 549.
- [131] P. Zou, R. Zhang, L. Yao, J. Qin, K. Kisslinger, H. Zhuang, H. L. Xin, *Adv. Energy Mater.* **2021**, 11, 2100982.
- [132] X. T. Zhang, J. X. Li, D. Y. Liu, M. K. Liu, T. S. Zhou, K. W. Qi, L. Shi, Y. C. Zhu, Y. T. Qian, *Energy Environ. Sci.* **2021**, 14, 3120.
- [133] P. Liu, W. Liu, Y. Huang, P. Li, J. Yan, K. Liu, *Energy Storage Mater.* **2020**, 25, 858.
- [134] S. H. Park, S. Y. Byeon, J.-H. Park, C. Kim, *ACS Energy Lett.* **2021**, 6, 3078.
- [135] F. Wan, J. Zhu, S. Huang, Z. Niu, *Batteries Supercaps* **2020**, 3, 323.
- [136] C. Zhang, J. Holoubek, X. Wu, A. Daniyar, L. Zhu, C. Chen, D. P. Leonard, I. A. Rodriguez-Perez, J. X. Jiang, C. Fang, X. Ji, *Chem. Commun.* **2018**, 54, 14097.
- [137] L. Wang, Y. Zhang, H. Hu, H. Y. Shi, Y. Song, D. Guo, X. X. Liu, X. Sun, *ACS Appl. Mater. Interfaces* **2019**, 11, 42000.
- [138] F. Wan, L. Zhang, X. Dai, X. Wang, Z. Niu, J. Chen, *Nat. Commun.* **2018**, 9, 1656.
- [139] W. Xu, K. Zhao, W. Huo, Y. Wang, G. Yao, X. Gu, H. Cheng, L. Mai, C. Hu, X. Wang, *Nano Energy* **2019**, 62, 275.
- [140] J. Zhao, J. Zhang, W. Yang, B. Chen, Z. Zhao, H. Qiu, S. Dong, X. Zhou, G. Cui, L. Chen, *Nano Energy* **2019**, 57, 625.
- [141] H. Qiu, X. Du, J. Zhao, Y. Wang, J. Ju, Z. Chen, Z. Hu, D. Yan, X. Zhou, G. Cui, *Nat. Commun.* **2019**, 10, 5374.
- [142] G. Wang, B. Kohn, U. Scheler, F. Wang, S. Oswald, M. Löffler, D. Tan, P. Zhang, J. Zhang, X. Feng, *Adv. Mater.* **2020**, 32, 1905681.
- [143] A. Mitha, A. Z. Yazdi, M. Ahmed, P. Chen, *ChemElectroChem* **2018**, 5, 2409.
- [144] A. Naveed, H. Yang, J. Yang, Y. Nuli, J. Wang, *Angew. Chem., Int. Ed.* **2019**, 58, 2760.
- [145] Q. Zhang, Y. Ma, Y. Lu, L. Li, F. Wan, K. Zhang, J. Chen, *Nat. Commun.* **2020**, 11, 4463.
- [146] F. Wang, O. Borodin, T. Gao, X. Fan, W. Sun, Han, A. Faraone, J. A. Dura, K. Xu, C. Wang, *Nat. Mater.* **2018**, 17, 543.
- [147] C. Zhong, B. Liu, J. Ding, X. Liu, Y. Zhong, Y. Li, C. Sun, X. Han, Y. Deng, N. Zhao, W. Hu, *Nat. Energy* **2020**, 5, 440.



Jiaxian Zheng is a master's student under the supervision of Prof. Hanfeng Liang at Xiamen University. His research mainly focuses on aqueous zinc-ion batteries, especially the development of high-performance Zn anodes.



Qiu Jiang is an associate professor in the School of Materials and Energy at the University of Electronic Science and Technology of China (UESTC). He obtained his Ph.D. at King Abdullah University of Science and Technology, Saudi Arabia. He is interested in developing functional nanomaterials for energy storage and conversion applications.



Zhengbing Qi is an associate professor at the School of Materials Science and Engineering at Xiamen University of Technology. He received his B.S. and Ph.D. degrees from the College of Chemistry and Chemical Engineering at Xiamen University. His current research interests include surface and coatings technology, functional thin films, and electrochemical energy storage.



Hanfeng Liang received his Ph.D. (2015) from Xiamen University, China. He joined Xiamen University as an associate professor in 2020 after postdoc at King Abdullah University of Science and Technology, Saudi Arabia. He currently serves as an associate editor of *Frontiers in Materials* and is on the (youth) editorial board of several journals. His research focuses on nanomaterials and functional coatings as well as their application in electrocatalysis and energy storage. He has published over 70 papers with >7500 citations (h-index 39).